PEAK LOAD OF ELECTRICITY DEMAND FORECAST USING MACHINE LEARNING AND ELECTRICITY GENERATION PLANNING

BY

MAY THAZIN PHUU WAI

A THESIS SUBMITTED IN PARTIAL FULFILLMENT OF THE REQUIREMENTS FOR THE DEGREE OF MASTER OF SCIENCE (ENGINEERING AND TECHNOLOGY)
SIRINDHORN INTERNATIONAL INSTITUTE OF TECHNOLOGY
THAMMASAT UNIVERSITY
ACADEMIC YEAR 2025

THAMMASAT UNIVERSITY

SIRINDHORN INTERNATIONAL INSTITUTE OF TECHNOLOGY

THESIS

BY

MAY THAZIN PHUU WAI

ENTITLED

PEAK LOAD OF ELECTRICITY DEMAND FORECAST USING MACHINE LEARNING AND ELECTRICITY GENERATION PLANNING

was approved as partial fulfillment of the requirements for
the degree of Master of Science (Engineering and Technology)

on November 12, 2025

Chairperson _____
(Assistant Professor Boonyarit Intiyot, Ph.D.)

Member and Advisor _____
(Associate Professor Aussadavut Dumrongsiri, Ph.D.)

Member and Co-advisor _____
(Associate Professor Chawalit Jeenanunta, Ph.D.)

Member _____
(Associate Professor Pisit Chanvarasuth, Ph.D.)

Director _____
(Associate Professor Kriengsak Panuwatwanich, Ph.D.)

Thesis Title	PEAK LOAD OF ELECTRICITY DEMAND FORECAST USING MACHINE LEARNING AND ELECTRICITY GENERATION PLANNING
Author	May Thazin Phuu Wai
Degree	Master of Science (Engineering and Technology)
Faculty/University	Sirindhorn International Institute of Technology/ Thammasat University
Thesis Advisor	Associate Professor Aussadavut Dumrongsiri, Ph.D.
Thesis Co-Advisor	Associate Professor Chawalit Jeenanunta, Ph.D.
Academic Years	2025

ABSTRACT

Short-term load forecasting plays a critical role in power system planning, operational scheduling, and economic dispatch. However, forecasting accuracy often deteriorates under irregular calendar conditions, such as weekends, public holidays, and bridging holidays, when load behavior deviates from typical daily patterns. This study proposes a two-stage hybrid forecasting framework that integrates calendar-aware classification with machine learning regression to improve day-ahead load prediction across diverse operating conditions. The methodology incorporates Random Forest (RF) classification to segment historical data using Month of Year (MoY), Day of Week (DoW), holiday, and bridging-holiday indicators, followed by RF regression to predict the 48 half-hourly loads for Thailand and the 24-hourly loads for France from 2019 to 2021. A linear interpolation mechanism is introduced to address insufficient samples in rare calendar categories.

Experimental results demonstrate that the proposed RF-RF framework consistently outperforms baseline methods, including Multiple Linear Regression (MLR), Support Vector Regression (SVR), Everyday classification, and Rule-based

classification across both countries. For Thailand, the hybrid model achieves the lowest average MAPE of 4.03% and RMSE of 4.47%, effectively capturing nonlinear seasonal and calendar-driven variations. For France, characterized by strong winter heating demand, the proposed method also yields superior performance, with MAPE 3.01% and RMSE 4.49%, confirming its generalizability across different climatic and load-profile regimes. The improvements are most pronounced on holidays and bridging holidays, where traditional models typically suffer from instability due to irregular consumption patterns.

Overall, this research demonstrates that integrating calendar-based segmentation with ensemble learning enhances pattern recognition, model robustness, and prediction accuracy. The proposed framework offers a scalable, interpretable solution for system operators seeking reliable short-term forecasting across diverse climatic contexts and complex calendar effects.

Keywords: Classification, Short-Term Load Forecasting, Machine Learning, Random Forest Classification, Calendar-Based Segmentation

ACKNOWLEDGEMENTS

First and foremost, I would like to express my heartfelt gratitude to my advisors, Assoc. Prof. Dr. Chawalit Jeenanunta and Assoc. Prof. Dr. Aussadavut Dumrongsiri, for their unwavering support, belief in my capabilities, and exceptional mentorship throughout this research. Their guidance, encouragement, and insightful feedback have been instrumental in shaping both the direction of this work and my academic growth. I am deeply grateful for the trust they placed in me and for the continuous motivation they provided, which enabled me to persevere through every challenge.

I would also like to thank my committee members, Assoc. Prof. Dr. Pisit Chanvarasuth and Asst. Prof. Dr. Boonyarit Intiyot, for their valuable comments and constructive suggestions that significantly improved the quality of this thesis.

My sincere appreciation extends to Thammasat University and the Sirindhorn International Institute of Technology (SIIT) for their generous support through the TISR Scholarship. This support has provided essential opportunities and resources that made my academic and research journey possible.

I am profoundly grateful to my family. My mother, grandparents and my sister have been my constant sources of strength, offering unconditional love, encouragement, and unwavering belief in me. Their support and sacrifices have sustained me throughout this journey, and this achievement is equally theirs. I also extend my heartfelt appreciation to SEVENTEEN, whose music brought comfort and be my strength during my lowest moments and reminded me to keep going when the path felt difficult.

Lastly, I would like to thank all my seniors, my friends, my research group, and everyone whom I may not be able to mention individually. Their kindness, guidance, and support in countless ways have enriched my experience and helped make this research possible.

May Thazin Phuu Wai

TABLE OF CONTENTS

LIST OF TABLES

LIST OF FIGURES

LIST OF SYMBOLS/ABBREVIATIONS

Symbols/Abbreviations	Terms
AI	Artificial Intelligence
ANN	Artificial Neural Network
B-Hol	Bridging holiday
CART	Classification and Regression Tree
CNN	Convolutional Neural Network
DL	Deep Learning
DoW	Day of week
EGAT	Electricity Generating Authority of Thailand
ENTSO-E	European Network of Transmission System Operators for Electricity
GRU	Gated Recurrent Unit
KPCA	Kernel Principal Component Analysis
LSTM	Long Short-Term Memory
MAPE	Mean Absolute Percentage Error
ML	Machine Learning
MLR	Multiple Linear Regression
MoY	Month of Year
MSE	Mean Squared Error
RF	Random Forest
RMSE	Root Mean Square Error
RNN	Recurrent Neural Network
SIIT	Sirindhorn International Institute of Technology
STLF	Short-Term Load Forecasting
SVR	Support Vector Regression
TU	Thammasat University

CHAPTER 1
INTRODUCTION

1.1 Electricity Load Forecasting

Electric load refers to any electrical device or component within an electric circuit that requires power to perform essential functions, such as lighting, heating, or operating machinery. It indicates the demand for electrical supply and is typically measured in watts (W) or kilowatts (kW).

Electricity load forecasting is the process of estimating future electricity demand based on historical load trends, weather conditions, and socioeconomic factors. This forecasting plays a crucial role in modern power system management. Accurate forecasts enable system operators to optimize generation scheduling, reduce operating costs, prevent blackouts, and enhance the overall efficiency and reliability of the power system.

Load forecasting can be categorized by prediction time frame into long-term, medium-term, and short-term forecasts. Among these, Short-Term Load Forecasting (STLF) focuses on predicting demand over a period ranging from a few hours to several days. For instance, STLF is vital for real-time operations, load dispatching, and market decision-making.

.

1.1.1 Electricity Load in the Power System

In a power system, the electricity load is the total electrical power demand from consumers, including residential, commercial, industrial, and other applications.

1. Residential loads are electricity requirements from residences, originating from lighting, appliances, and heating or cooling systems. In residential load, there are daily cycles where there is greater demand in the morning and then in the evening, and seasonal fluctuations based on heating/cooling needs
2. Commercial loads include businesses, offices, and malls that have demand for lighting, HVAC systems, and equipment like elevators. These loads follow business hours, with higher consumption during the day, but may also extend into evenings or nights, depending on the type of business.

3. Industrial loads are typically high and continuous, with peaks during production changes in factories and plants where they use large machinery, motors, and high-energy equipment like furnaces. These loads are less influenced by time of day but depend on operational schedules and machinery use.

1.2 Nature of Load

The nature of the electricity load refers to the pattern of electricity load consumption over time, which changes due to various factors. Understanding these patterns is key to predicting load. This is a simplified explanation of the key aspects:

1) Changes Over Time

- Daily Variations: Electricity use fluctuates during the day. There are typically higher demands in the morning and evening, when people use appliances for heating, cooling, or cooking.
- Seasonal Variations: Demand is higher during hot summers (due to air conditioning) or cold winters (due to heating).
- Weekly Variations: Electricity use is usually lower on weekends compared to weekdays, except in industries that operate every day.
- Holidays and Special Days: National holidays, weekends, and bridging holidays (days between weekends and holidays) can cause unusual shifts in demand, as people's work and leisure patterns change.

2) Peak and Off-Peak Times

- Peak Load: This is the highest demand for electricity during a specific time, usually during high-use periods (e.g., summer afternoons or winter mornings).
- Off-Peak Load: This is the lower demand during periods when fewer people are using electricity, such as late at night or early in the morning.

3) Load Patterns

- Base Load: This is the steady minimum level of electricity needed throughout the day, usually for essential activities like lighting and refrigeration.
- Peak Load: These are the sharp increases in demand during certain times of the day or special events, which require extra power generation capacity.
- Load Factor: This is a measure of how steady or variable electricity use is. A high load factor means electricity is used consistently, while a low load factor indicates

significant demand fluctuations.

4) Factors that Influence Load

- Weather: Extreme temperatures (hot or cold) can cause spikes in electricity demand due to heating or cooling needs.
- Economic and Social Factors: Changes in population, economic activity, and lifestyle can also affect electricity demand. Special events, such as festivals or public holidays, can cause unexpected surges in demand.
- Calendar Effects: The electricity demand can change on public holidays, weekends, or bridging holidays due to altered work and leisure schedules.

1.3 Electricity Load Profile

Load profiles, typically visualized using line graphs or histograms, provide a comprehensive overview of electricity consumption patterns over a defined period. Analyzing load profiles is essential for understanding load usage dynamics, identifying peak demand periods, and assessing load variability. This process involves examining load profile trends to uncover patterns and variations in electricity consumption, enabling a deeper understanding of load characteristics and the factors influencing them.

1.3.1 Relationship between Peak Load and Seasonal Trends

The historical datasets used in this study were obtained from the Electricity Generating Authority of Thailand (EGAT) and the French Transmission System Operator (ENTSO-E). The Thailand dataset comprises net load measured at 30-minute intervals, with 48 periods per day, from 2019 to 2021. In contrast, the French dataset provides hourly load measurements with 24 periods per day for the same three-year period. Peak load represents the maximum electricity demand recorded within each daily cycle and is closely tied to climatic conditions, economic activity, and behavioral patterns.

Seasonal analysis reveals distinct differences between the two countries. Thailand, located in a tropical climate zone, exhibits substantial temperature-driven variability, especially during the hot season when cooling demand intensifies. Conversely, France, in a temperate climate, experiences peak loads primarily in winter

due to heating demand, with lower consumption during summer. Exploratory data analysis (EDA) of both datasets by examining daily load patterns (Monday-Sunday), seasonal quarters, and yearly behavior (2019-2021), which highlights how climate, working schedules, and cultural events shape electricity consumption. Thailand demonstrates pronounced summer-driven peaks, whereas France shows winter-dominant high loads with apparent seasonal shifts.

1.3.2 Daily Load Profile

Daily load curves for both Thailand and France, as illustrated in Fig. 1.1, show consistent day-of-week patterns but differ in their intensity and timing. In Thailand, weekdays exhibit higher, more stable daytime loads, driven by commercial, industrial, and government operations. These loads typically peak in the late afternoon due to the combined effects of heat and business-hour consumption. Weekends, particularly Sundays, show significantly lower overall demand due to reduced economic activity.

In France, weekday load patterns also reflect standard working schedules, with clear morning and evening peaks associated with commuting, heating, and household activities. Weekend loads, especially on Sundays, drop noticeably as commercial activities diminish. However, compared with Thailand, France's curves display stronger morning peaks and smoother midday consumption, reflecting climate differences and different patterns of residential and heating use.

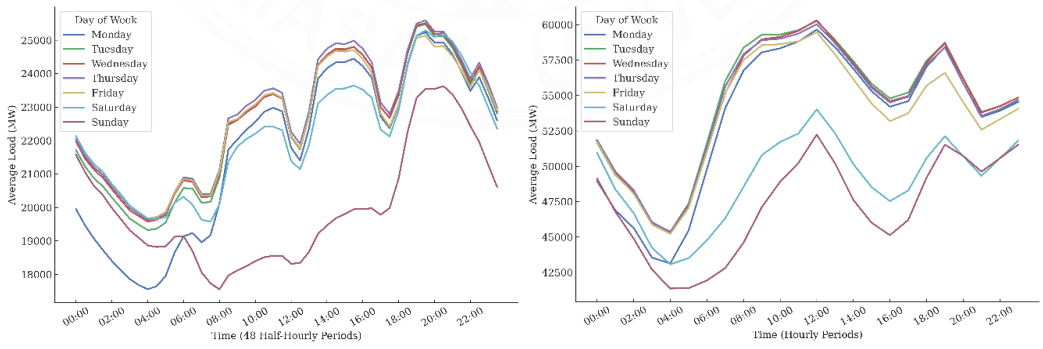

(i) (ii)

Figure 1.1 Average Daily Load Profile by Day of Week for (i) Thailand and (ii) France

1.3.3 Seasonal Load Profile

Seasonal load variations reveal contrasting consumption behaviors between Thailand and France, reflecting their distinct climatic conditions. As shown in Fig. 1.2, Thailand's load is highest during the hot season (April-June), when temperatures peak, and cooling demand intensifies. The rainy season (July-September) sustains high consumption due to persistent humidity, while cooler months (January-March) show comparatively lower loads except for short holiday-driven spikes. Electricity demand gradually declines toward the end of the year, though festive activities in December create noticeable increases.

In France, the seasonal trend follows an opposite pattern. Electricity demand is highest during winter (January-March and October-December), driven by heating requirements. As temperatures rise in late spring and summer, overall consumption drops significantly due to reduced heating needs and limited reliance on air-conditioning. Unlike Thailand, France does not experience substantial summer peaks. These contrasting profiles underscore how climate conditions shape national load behavior. Thailand peaks in the hottest months due to cooling demand, while France peaks in the coldest months due to heating demand.

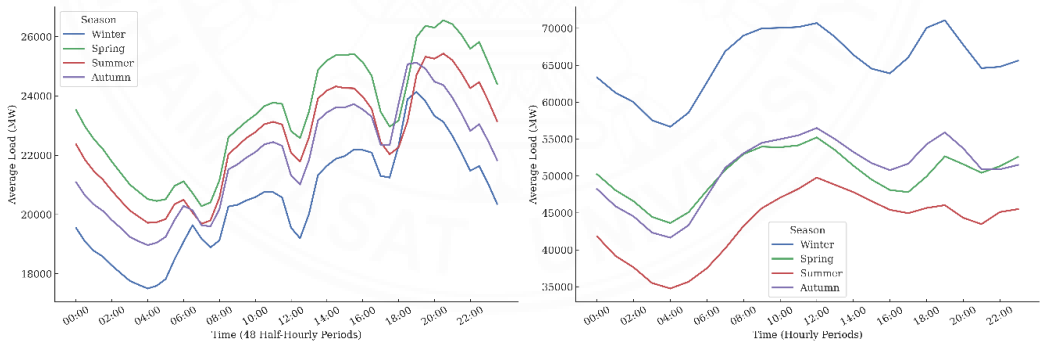

(i) (ii)

Figure 1.2 Seasonal Peak Load Variation in (i) Thailand and (ii) France

1.3.4 Yearly Lod Profile

Figure 1.3 illustrates the annual load patterns for Thailand and France, highlighting the influence of various factors, including climate conditions and socio-economic disruptions such as the COVID-19 pandemic. In Thailand, the load exhibits typical peaks in the morning and evening, reflecting the workday routine in 2019.

However, the implementation of work-from-home measures in 2020 led to a decrease in morning peaks and an increase in midday loads. By 2021, traditional load patterns began to re-emerge.

In France, similar pandemic-related effects were observed, but with more pronounced trends during the winter months. Heating demand emerged as the primary driver, leading to significant winter peaks in almost all individual years. Notably, there were considerable reductions in load during the 2020 lockdowns, followed by a recovery in 2021. Overall, these trends underscore the responsiveness of long-term load behavior to both climatic seasonality and societal changes.

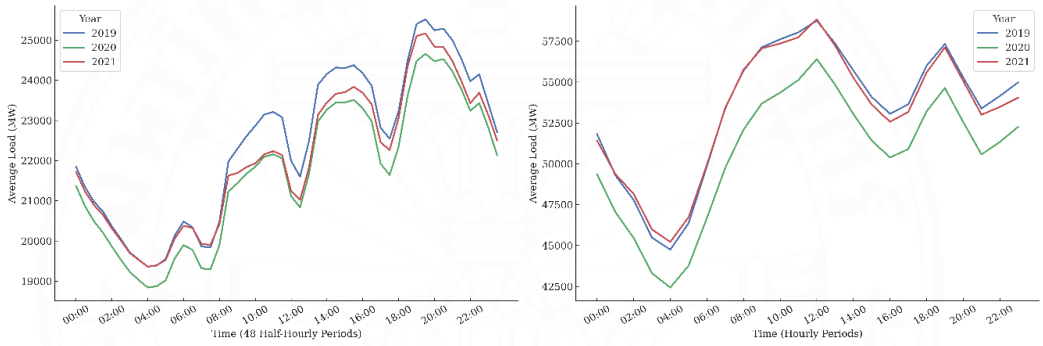

(i) (ii)

Figure 1.3 Annual Peak Load Trend for (i) Thailand and (ii) France (2019-2021)

1.4 Electricity Load Forecasting

Load forecasting is essential for effective planning and development of an electric power system. Essentially, it involves predicting future electricity load based on a variety of factors. This process requires analyzing historical data, identifying patterns, and considering external influences that affect electricity consumption.

The load forecasting can cover a wide range of timeframes, from a few hours to several years ahead. To achieve accurate predictions, load forecasting involves several key steps. First, data must be collected and preprocessed. Then, appropriate models are selected and trained using the gathered information. Finally, the performance of these models is evaluated using metrics such as the Mean Absolute Percentage Error (MAPE) and Root Mean Square Error (RMSE), which help determine how accurately the forecasts align with actual demand.

1.4.1 Types of Load Forecasting

Load forecasting is the process of predicting the volume and frequency of electricity demand over extended periods, as well as its distribution. It can be categorized by time frames, purposes, and methodologies into Short-Term Load Forecasting (STLF), Medium-Term Load Forecasting (MTLF), and Long-Term Load Forecasting (LTLF).

STLF predicts electricity demand over short time intervals, typically ranging from a few hours to a few days. Peak load represents the highest electricity demand during a specific period. Temperature is a critical feature influencing electricity demand, especially for cooling or heating. It is an independent variable that captures the effects of seasonal and daily temperature on load patterns. Hour of Day represents the specific time of day (e.g., 0:00, 1:00). Weekdays indicate whether a day is a weekday (e.g., Monday-Friday). It helps to distinguish between typical working days and other days. Weekend is a feature indicating whether a day is a weekend (e.g., Saturday and Sunday). It captures variations in electricity usage patterns during non-working days. Holiday is a feature that indicates whether a day is a public holiday. It captures special consumption patterns during holidays. Bridging Holiday indicates whether a day falls between a holiday and a weekend, or between two holidays. These variables are commonly used in machine learning models to improve the accuracy of electricity demand forecasting. By employing predictive models such as machine learning algorithms or statistical regressions, these variables can be analyzed to determine their relationships. The anticipated outcome is a reliable forecast of electricity demand at specific points in time, enabling energy companies to plan their energy supply effectively.

1.4.2 Load Forecasting Models

Load forecasting models are predictive tools used to estimate electricity load over a specified time horizon. They can be classified into two main categories: traditional statistical models and artificial intelligence-based models.

Traditional statistical models, such as Linear Regression, Time Series Models (ARIMA, SARIMA), and Exponential Smoothing, rely on simpler methods to forecast

load based on historical data. Linear regression predicts load based on linear relationships with variables such as temperature or time of day, while time-series models like ARIMA and SARIMA capture trends and seasonality in the data. Exponential smoothing assigns exponentially decreasing weights to past observations, making it helpful in forecasting data with trends or seasonal patterns.

AI-based models, including Machine Learning (ML) Models and Deep Learning (DL) Models, handle more complex, non-linear patterns in large datasets. Machine learning models such as Support Vector Regression (SVR), Artificial Neural Networks (ANN), Random Forest (RF), and Gradient Boosting (XGBoost, CatBoost, LightGBM) excel in capturing intricate relationships and patterns in data. Deep learning models such as Recurrent Neural Networks (RNNs), Long Short-Term Memory (LSTMs), Convolutional Neural Networks (CNNs), and Transformer Models are particularly effective at modeling sequential data and long-range dependencies, achieving high accuracy in forecasting. While traditional models are more straightforward, more interpretable, and work well with smaller datasets, AI-based models require larger datasets. Still, they are more flexible, offering higher accuracy and the ability to manage complex, non-linear relationships in the data.

1.5 Research Problem

Despite considerable progress in ML-based short-term load forecasting, accuracy remains limited by three persistent challenges. First, forecast errors remain large during holidays and bridging holidays, as these days exhibit irregular, unpredictable consumption patterns that differ sharply from those on regular weekdays and weekends. Second, many existing models fail to incorporate calendar-aware segmentation before training and therefore assume that the relationship between input features and electricity demand is consistent across all days, even though actual consumption varies by calendar type. Third, holidays and bridging holidays occur only a few times per year, resulting in insufficient training samples that prevent models from effectively learning their unique behavior.

As a result, models trained on aggregated data often struggle during special days or high-variability periods, particularly in months like April and December, ultimately reducing forecasting reliability and increasing operational and generation planning

costs. This research aims to develop accurate and reliable forecasting models to predict peak load under varying patterns. This helps with better planning and management of power systems.

1.6 Research Objectives

This study aims to improve the accuracy of daily peak load forecasting in Thailand by developing a two-stage hybrid framework. The specific objectives are:

1. To develop five calendar-based classification approaches: Everyday, Rule-based, CART, and Random Forest (RF) Classification.
2. To apply three forecasting models: Multiple Linear Regression (MLR), Support Vector Regression (SVR), and Random Forest Regression (RF) within each classified subset.
3. To propose fallback strategies for handling days with insufficient training samples.
4. To evaluate and compare forecasting performance across models and classification strategies using MAPE and RMSE.
5. To analyze performance across months and calendar types, highlighting high-error periods and model robustness.

1.7 Research Contribution

This research makes a practical contribution to both Thailand and France, showing that even minor improvements in short-term forecasting accuracy can lead to substantial benefits across the entire system. For instance, in Thailand, where annual electricity consumption is projected to reach 214,469 GWh in 2024, a mere 1% improvement in the Mean Absolute Percentage Error (MAPE) could result in about 2,144 GWh per year of better-scheduled energy production. This would lead to a reduction of 214 GWh per year in reserve dispatch, translating to nearly 900 million THB in annual savings on operating costs.

Similarly, in France, which consumes over 450,000 GWh annually and experiences significant load fluctuations mainly due to electric heating, a 1% increase in forecasting accuracy could yield approximately 4,500 GWh per year in more precise scheduling. This improvement could save between 315 and 405 million EUR per year in balancing costs.

Across both countries, the proposed Random Forest-based classification and forecasting framework not only enhances accuracy, particularly on challenging calendar days, but also improves economic dispatch, reduces system stress, and supports the long-term reliability of the power grid.

CHAPTER 2
REVIEW OF LITERATURE

2.1 Related Works and Models

2.1.1 Random Forest and Ensemble-Based Machine Learning Models

Alquthami et al. conduct a rigorous comparative analysis of various machine learning algorithms for STLF using a real-world dataset from a Saudi Arabian utility(Alquthami et al., 2022). The study evaluates the performance of Support Vector Machines (SVM), Random Forests (RF), Artificial Neural Networks (ANN), and deep learning models, including Gated Recurrent Units (GRU) and standard Recurrent Neural Networks (RNN). Their key finding is that the Random Forest algorithm and the GRU deep learning model consistently provide the highest accuracy, demonstrating the lowest Mean Absolute Percentage Error (MAPE) and Root Mean Square Error (RMSE), thereby validating the robustness of both ensemble and advanced neural network methods for this task.

Dudek provides a comprehensive and systematic study dedicated entirely to the Random Forest (RF) algorithm for STLF. Rather than hybridizing, this paper offers a deep dive into the model's architecture and parameters, including the number of trees, input variable configurations, and tree depth. The study rigorously analyzes how these parameters affect forecasting accuracy (Dudek, 2022). It concludes that a well-tuned RF is a highly effective, robust, and simple-to-implement standalone solution for STLF, often outperforming more complex models.

Fan et al. explores a novel application of Random Forests to construct a multivariable response surface for STLF (Fan et al., 2022). Instead of using RF for direct time-series prediction, they use it to model the complex, non-linear relationships among multiple input variables (such as temperature, humidity, and time of day) and the resulting load. This RF-generated surface serves as a sophisticated regression tool that accurately maps inputs into outputs, providing a new framework for using ensemble methods in forecasting.

Gao et al. focus on improving the standard Random Forest algorithm specifically for ultra-short-term electricity load forecasting (e.g., 15-minute or 30-minute intervals) (Gao et al., 2023). Their improved random forest model optimizes hyperparameters and feature selection using a metaheuristic algorithm. The goal is to create a model that is not only accurate but also computationally efficient, which is a critical requirement for high-frequency, real-time forecasting.

Khan et al. address the dual challenges of multiple load types (e.g., residential, commercial, industrial) and limited sampling data. They propose an effective ensemble learning model that trains distinct machine learning models (e.g., SVM, RF, k-NN, ANN) and combines their predictions using weighted voting. This ensemble method proves more stable and accurate than any single model, particularly in sparse-data environments(Khan et al., 2024).

Magalhães et al. focus on enhancing the Random Forest model through a dual-optimization process (Magalhães et al., 2024). Their paper proposes an STLF model based on an optimized Random Forest, in which both the model's internal hyperparameters and the optimal feature subset are tuned simultaneously, often using a genetic algorithm or similar methodology. This approach systematically explores the configuration space to identify high-performing combinations of features and parameters.

Srivastava et al. present a hybrid model that places strong emphasis on feature selection. The core of their methodology is a hybrid feature selection process that combines an elitist genetic algorithm with Random Forest(Srivastava, 2020). This two-step process aggressively removes irrelevant or redundant features, and the resulting feature set is then fed into an M5P machine learning algorithm, a model tree that uses linear regression at its leaves for the final day-ahead forecast.

Wai-Keung Yiu et al. introduce a novel ensemble model based on Regularized Greedy Forest (RGF). RGF is a tree-based ensemble algorithm, similar to Gradient Boosting or Random Forest, but it grows trees using a greedy optimization process with built-in regularization to prevent overfitting. The paper proposes an ensemble of RGF models and shows that this approach achieves higher accuracy and better generalization than more common ensemble methods, such as XGBoost (Wai-Keung Yiu et al., 2024).

Sankalpa et al. propose an ensemble-based STLF model that combines predictions from multiple individual models to produce a more accurate and stable final forecast (Sankalpa et al., 2022). A key aspect of their work is the emphasis on rigorous validation and cross-validation, ensuring that the ensemble's superior performance is statistically significant and not merely due to overfitting to a particular test set.

2.1.2 Hybrid Deep Learning and Machine Learning Models

Chen et al. argue that forecasting accuracy is heavily dependent on the quality of input data and features. They propose a combination forecasting method that begins with advanced feature extraction, using techniques like Kernel Principal Component Analysis (KPCA) and Singular Spectrum Analysis (SSA) to decompose the original load data and remove noise (Chen et al., 2024). This cleaned and feature-enhanced data is then fed into a hybrid deep learning model (e.g., GRU-TCN), demonstrating that sophisticated data pre-processing can significantly improve the predictive power of subsequent forecasting models.

Cui et al. present a sophisticated multi-stage hybrid model for STLF. The methodology first addresses feature engineering by employing a combined XGBoost–RF feature selection technique to identify and isolate the most influential input variables. The optimized feature set is then fed into a deep learning architecture combining a Convolutional Neural Network (CNN) and a Gated Recurrent Unit (GRU) (Cui et al., 2024). The CNN layer extracts spatial features from the inputs, while the GRU layer models the temporal dependencies, creating a potent hybrid that captures complex temporal patterns.

Fang et al. propose a hybrid model for ultra-short-term load prediction that combines LSTM and Random Forest (LSTM–RF). In this architecture, the LSTM network is used to model the primary time-series component and capture the main trend of the load data(Fang et al., 2022). The Random Forest model is then employed to predict residual error, i.e., the element of the forecast that the LSTM failed to capture. The final, more accurate prediction is the sum of the LSTM's forecast and the RF's residual correction.

Fan et al. introduce a complex, multi-stage hybrid model designed for high-accuracy STLF (Fan et al., 2021). Their model integrates Support Vector Regression

(SVR), known for its ability to handle non-linear data, with Grey Catastrophe modeling, which addresses data uncertainty, and Random Forests. In this framework, RF is used to refine predictions or select features, complementing the SVR model. This three-part hybridization aims to leverage the strengths of each method to produce a final forecast that is more robust and accurate than any single model.

Liu et al. propose a highly structured, three-stage hybrid model. First, the historical load data are clustered using an improved fuzzy C-means algorithm to automatically group days into distinct patterns (e.g., high-load weekdays, low-load weekends). Second, Random Forest is used to select features within each cluster. Finally, a separate Deep Neural Network (DNN) is trained for each data cluster, yielding a set of specialized models that together produce a more accurate final forecast (F. Liu et al., 2021).

Liu et al. leverage state-of-the-art deep learning architectures by proposing a model combining time-series clustering with a Transformer network. Similar to other clustering-based methods, their approach first groups days with identical load profiles. It then applies to a Transformer model with a self-attention mechanism to generate the forecast (Y. Liu et al., 2025). This allows the model to capture long-range and complex temporal dependencies in the data that simpler RNNs or LSTMs might miss.

Veeramsetty et al. propose a hybrid deep learning model that combines Random Forest (RF) and a Gated Recurrent Unit (GRU). In this architecture, RF handles static, non-temporal features (e.g., day of week or weather) and performs feature importance analysis, while the GRU models complex time-series dependencies (Veeramsetty et al., 2022). The outputs of both models are combined to exploit the feature-handling strength of RF and the temporal-modeling strength of GRU.

Yamasaki et al. focus on optimized hybrid ensemble learning approaches for very short-term load forecasting (VSTLF). Their framework combines predictions from multiple models (e.g., RF, SVR, ANN) and uses a metaheuristic optimization algorithm to find the optimal weights for blending their forecasts. This automated weighting process produces a custom-tuned ensemble that outperforms its individual components for high-frequency (e.g., 5-minute) predictions (Yamasaki et al., 2024).

2.1.3 Probabilistic and Risk-Aware Forecasting

Aprillia et al. shift the focus from traditional point forecasting to probabilistic forecasting, which is critical for risk assessment. They propose an Optimal Quantile Regression Random Forest (QRRF) model (Aprillia et al., 2021). This method not only predicts the expected load but also generates a range of outcomes (quantiles), creating a prediction interval. This approach allows grid operators to quantify the risk and uncertainty associated with their forecasts, representing a significant improvement over the deterministic method.

Zhang et al. contribute to probabilistic load forecasting by proposing a hybrid LSTM-based Twin Support Vector Regression (TWSVR) model (Zhang et al., 2025). The LSTM component is used to extract and model temporal patterns in the time-series data, and the processed information is fed into a TWSVR model, an advanced variant of SVR. The method is particularly effective at generating both point forecasts and predictive intervals (upper and lower bounds), thereby enabling practical risk assessment.

2.1.4 Meta-Learning, Clustering, and Transferability

He et al. tackle the challenging problem of household load forecasting, where training data for a new house are minimal. They propose a transferable Model-Agnostic Meta-Learning (MAML) approach (He et al., 2022). This technique involves training a meta-model on a large set of households, which can then be rapidly and accurately adapted to a new household with only a few data points, thereby overcoming the cold-start problem that often affects individualized forecasting.

Pinheiro et al. (Pinheiro et al., 2023)present a systematic literature review (SLR) that maps the STLF research field. Rather than proposing a new model, they synthesize and organize existing literature. Their systematic approach categorizes studies by forecasting target, ranging from the entire grid (system level) to individual secondary substations (neighborhood level). This analysis identifies trends, popular methodologies (such as RF and LSTM), and remaining research gaps across different levels of the power grid.

Madhukumar et al. present a case study on STLF for a university campus. This type of institutional load is unique, as it is driven by factors (e.g., academic calendars,

class schedules, laboratory usage) that differ significantly from typical residential or commercial patterns. The paper evaluates various regression models to identify the best fit for this specific and challenging load profile, highlighting the need for tailored models rather than a one-size-fits-all approach (Madhukumar et al., 2022).

2.1.5 Calendar, Holiday, and Special-Day Aware Forecasting

Lahouar and Slama(Lahouar & Ben Hadj Slama, 2015), an earlier but foundational paper in this list, demonstrates the power of combining machine learning with domain knowledge. They propose a day-ahead forecast model that combines Random Forest with expert input selection. This two-stage process involves, first, using human expertise to identify a set of potentially relevant features such as weather and calendar data, and second, using the built-in feature importance mechanism of Random Forest to select the optimal feature subset. This yields a simple yet highly effective model.

Lee provides a focused analysis on forecasting daily peak load in South Korea, a metric that is often more critical for grid stability than the complete 24-hour profile. The study evaluates a suite of regression-based methods, ranging from classical multiple linear regression to more advanced machine learning models such as SVR and RF(Lee, 2022). It serves as a practical case study for comparing the efficacy of these approaches in predicting maximum daily load.

López et al. directly address the special-day or holiday problem, which is a key gap in many STLF studies. Using a Spanish dataset, their work focuses exclusively on classifying special days (e.g., national holidays, regional holidays, bridging holidays). They argue that accurately identifying these days before forecasting is a critical prerequisite (López et al., 2019). Once they are classified, specialized models or similar-day methods can be applied, but the classification step itself remains a significant, unsolved challenge for forecasters.

Son et al.(Son et al., 2022), similar to López et al. (López et al., 2019), directly tackle the holiday forecasting problem. Their proposed method is based on modifying the load profiles of identical days. When forecasting a holiday, the model first identifies similar past days (e.g., previous occurrences of the same holiday or other holidays with similar characteristics) and then modifies these historical profiles, such as scaling them

up or down based on recent trends, before combining them to create the final day-ahead forecast.

Thu Tun et al. focus on the critical pre-processing step of data cleaning. They propose a rule-based classification method and an outlier-replacement approach to improve data quality before forecasting. This involves creating a set of rules to automatically identify anomalous data points, such as measurement errors or special days like holidays (Thu Tun et al., 2023). Once identified, these outliers are replaced with more representative values, leading to a cleaner dataset that improves the accuracy of subsequent forecasting models.

Zhou et al. address the dual problem of forecasting both the daily maximum load and its time of occurrence. Their model first uses the Hausdorff distance, a metric for measuring the distance between two sets of points, to identify similar days in the past (Zhou et al., 2021). Once these similar days are found, an Elastic Net regression model (a linear regression variant that combines L1 and L2 regularization) is trained on this subset to predict both the peak load and its timing.

Table 2.1 Summary of Related Short-Term Load Forecasting Literature

Author (Year)	Journal	Q	Forecasting Period	Data Resolution	Forecast Horizon	Classification Model	Forecasting Model	Inputs Used	Accuracy Metrics	Research Gap
Alquthami et al. (2022)	IEEE Access	Q1	STLF	Not specified	1-hour ahead	None	RF, SVR, ANN, Linear Regression	Load, temperature	MAPE, RMSE	No calendar/day-type classification
Aprillia et al. (2021)	IEEE Trans Smart Grid	Q1	STLF	Hourly (24 periods)	Day-ahead	None	QRF	Load, temperature	Pinball loss, MAPE	No special-day or B-Hol classification
Chen et al. (2024)	IEEE Access	Q1	STLF	Not specified	1-hour ahead	None	RF (feature extraction)	Load features	RMSE, MAPE	No day-type classification
Cui et al. (2024)	Processes	Q1	STLF	Not specified	30-min ahead	None	CNN–GRU + XGBoost + RF	Load, weather	MAPE, RMSE	Deep models do not segment days
Dudek (2022)	Energies	Q1	STLF	Hourly (24 periods)	1-hour ahead	None	RF	Lag load	MAPE, RMSE	RF not used as a classifier
Fang et al. (2022)	J Phys Conf Ser	Q2	U-STLF	Not specified	15-min ahead	None	LSTM + RF	Load	RMSE	No calendar segmentation
Fan et al. (2021)	Utilities Policy	Q1	STLF	Hourly (24 periods)	1-hour ahead	None	SVR + Grey System + RF	Load, weather	MAPE, RMSE	No holiday/B-Hol segmentation
Fan et al. (2022)	IJEPES	Q1	STLF	Not specified	1-hour ahead	None	RF	Load, time features	RMSE	No classification

Gao et al. (2023)	AIP Advances	Q1	U-STLF	Not specified	5 min ahead	None	IRF	Load	RMSE	No calendar features
He et al. (2022)	IEEE TPS	Q1	STLF	Not specified	1-hour ahead	None	MAML	Load	MAE, RMSE	No calendar awareness
Khan et al. (2024)	IEEE Access	Q1	STLF	Not specified	1-hour ahead	Cluster segmentation	Voting Ensemble (RF, SVM, KNN, ANN)	Load, cluster ID	RMSE, MAE	Not calendar-based
Lahouar & Slama (2015)	ECM	Q1	STLF	Hourly (24 periods)	Day-ahead	None	RF	Load, weather	MAPE	No day-type segmentation
Lee (2022)	Sustainability	Q1	STLF	Daily	Day-ahead	None	MLR	Load, weather	MAPE	No ML classification
Liu et al. (2021)	IEEE Access	Q1	STLF	Hourly (24 periods)	1-hour ahead	FCM	RF + DNN	Load, weather	MAPE	Clustering not calendar-based
Liu et al. (2025)	Electronics	Q1	STLF	Not specified	1-hour ahead	K-Shape Clustering	Transformer NN	Load clusters	RMSE	No holiday/B-Hol
López et al. (2019)	Energies	Q1	STLF	Hourly (24 periods)	Day-ahead	Manual Holiday Classification	Linear Regression	Load, calendar	MAPE	No ML classifier
Magalhães et al. (2024)	Energies	Q1	STLF	Not specified	1-hour ahead	None	Optimized RF	Load	RMSE	RF only; no two-stage approach

Madhukumar et al. (2022)	IEEE Access	Q1	Campus STLF	15-min (96 periods)	15 min ahead	None	MLR, SVR, RF	Load	MAPE	No calendar segmentation
Pinheiro et al. (2023)	Applied Energy	Q1	STLF	Not specified	1-hour ahead	Hierarchical Clustering	RF, SVR, ANN	Load	RMSE	No calendar grouping
Sankalpa et al. (2022)	Energies	Q1	STLF	Hourly (24 periods)	1-hour ahead	Simple manual	Ensemble (RF + GBM + ANN)	Load	MAPE	No ML-based classification
Son et al. (2022)	IEEE Access	Q1	STLF (holidays)	Hourly (24 periods)	Day-ahead (holidays)	Similar day	MLR/SVR	Load profiles	RMSE	No ML classifier; no B-Hol
Srivastava et al. (2023)	Energies	Q1	STLF	Hourly (24 periods)	Day-ahead	None	M5P + GA + RF	Load	MAPE	No day-type grouping
Thu Tun et al. (2023)	APPEEC	Q2	STLF	30 mins (48 periods)	Day-ahead	Rule-based	MLR, SVR, XGB, NN	Load, calendar	MAPE	Not ML classification
Veeramsetty et al. (2022)	Electrical Engineering	Q1	STLF	Not specified	1-hour ahead	None	RF + GRU	Load	RMSE	No calendar segmentation
Yiu et al. (2024)	IEEE Access	Q1	STLF	Not specified	30-min ahead	None	RGF	Load	MAPE, RMSE	Uniform for all days
Yamasaki et al. (2024)	IJEPES	Q1	VSTLF	30 mins (48 periods)	30-min ahead	None	Hybrid Ensemble (GBM + RF + DL)	Load	RMSE	No day-type modeling

Zhang et al. (2025)	IEEE TNNLS	Q1	STLF	Not specified	1-hour ahead	None	Twin SVR + LSTM	Load, weather	CRPS, RMSE	No calendar segmentation
Zhou et al. (2021)	AEEES	Q2	STLF	Daily	Day-ahead	None	Elastic Net	Load	RMSE	No classification

CHAPTER 3
METHODOLOGY

In this research, two historical electricity load datasets are used: Thailand's load dataset from the Electricity Generating Authority of Thailand (EGAT) and France's national load dataset obtained from ENTSO-E. The Thailand dataset covers five regions: the Central area, Bangkok, the South, the North, and the North-East. It provides highly granular insights into consumption behavior, differentiated by day type such as weekday, weekend, holiday, and bridging holiday, and influenced by Thailand's tropical climate, which drives pronounced seasonal peaks during hot months.

In contrast, the French dataset comprises hourly national load values, with 24 periods per day, for the same three-year timeframe. It reflects demand patterns shaped by a temperate climate, strong winter heating needs, and clear weekday-weekend distinctions. By integrating the datasets from Thailand and France, we can compare climate-driven load characteristics and enhance the robustness and generalizability of our forecasting framework across different power systems. We derive two-dimensional quantitative features, including load, lagged load variables, and calendar indicators, using traditional statistical methods and modern machine learning models. Model performance is assessed using the Mean Absolute Percentage Error (MAPE) and Root Mean Squared Error (RMSE), providing reliable and comprehensive metrics for short-term load forecasting. The overall forecasting methodology comprises four key components: data preprocessing, calendar-based classification, model development, and performance evaluation.

3.1 Overview of the Proposed Framework

The proposed forecasting framework employs a two-stage hybrid architecture designed to enhance the accuracy of short-term load forecasting in both Thailand and France. In the initial preprocessing stage, we address missing data and gather relevant features, including the Month of Year, Day of Week, Holiday indicators, Bridging Holiday indicators, and lagged load data. These processed datasets are then partitioned

into training and testing sets by day type to account for behavioral differences across calendar patterns.

This step is essential because Thailand and France show different behavioral load patterns. In Thailand, load trends are primarily driven by cooling demand, with pronounced afternoon peaks and high sensitivity to holidays. In contrast, France's load is largely heating-driven, characterized by a strong winter peak and notable variations between weekdays and weekends.

3.2 Calendar-Based Classification Methods

3.2.1 Everyday Classification

The Everyday Classification approach serves as the baseline classification method, in which each test day is forecasted using a fixed number of previous training days, regardless of their calendar type. In this study, behavioral shifts in demand driven by social or economic factors, such as reduced activity during holidays or increased demand, exhibit strong short-term temporal continuity, meaning recent load behavior provides valuable information for near-future predictions. While this approach is straightforward to implement, it does not differentiate between day types such as weekdays, weekends, or holidays. Consequently, it may not fully capture behavioral shifts in demand driven by social or economic factors, such as reduced activity during holidays or increased demand on workdays. Nonetheless, Everyday Classification provides a valuable benchmark against which the effectiveness of more advanced classification methods can be compared.

3.2.2 Rule-Based Classification

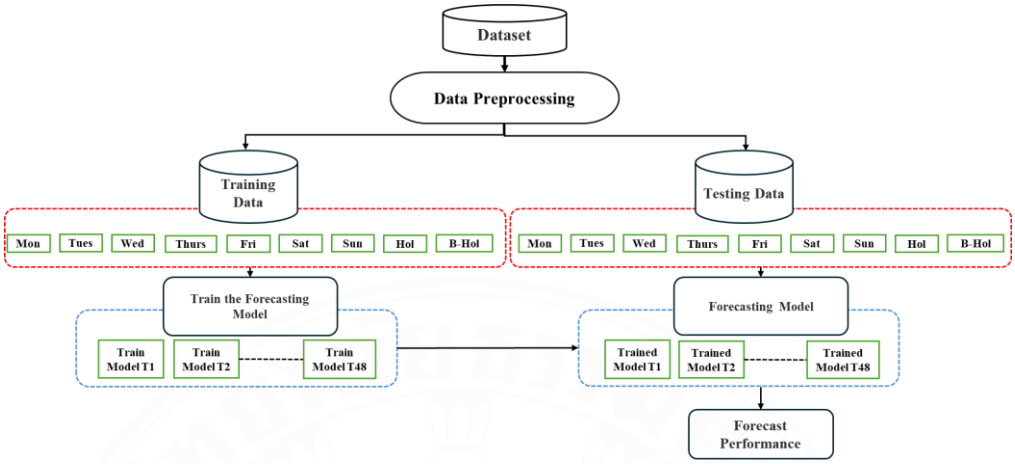

Figure 3.1 Forecasting Framework with Rule-Based Classification

The Rule-Based Classification method extends the Everyday approach by explicitly incorporating day-type segmentation. This classification ensures that the training data used for forecasting possess similar load patterns, reflecting both countries' unique calendar dynamics and cultural events. For example, national holidays in Thailand, such as Songkran or New Year's Eve, typically exhibit significantly lower electricity demand due to reduced industrial and commercial operations. By training forecasting models on samples of the same-day type, Rule-Based Classification enhances the contextual relevance of the training dataset. It reduces forecasting bias caused by mismatched temporal patterns.

3.2.3 CART Classification

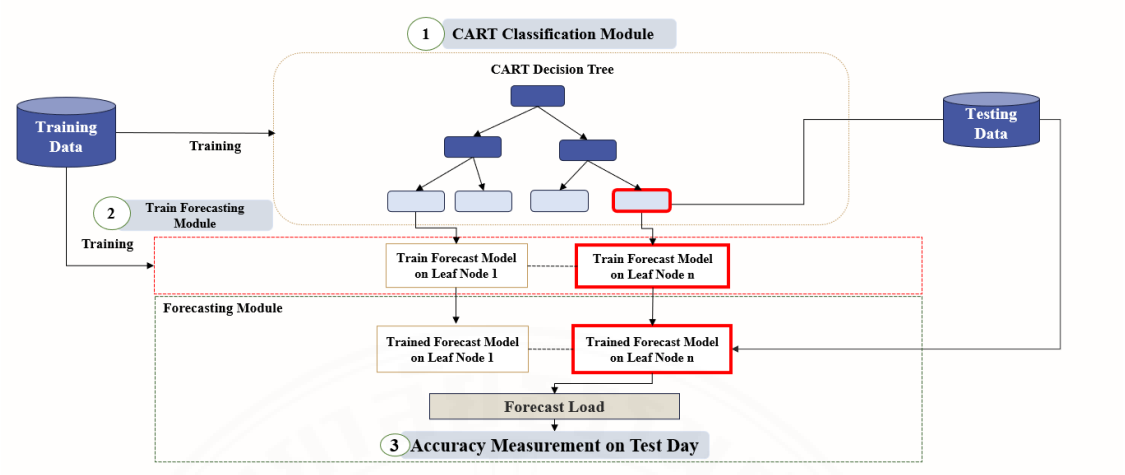

Figure 3.2 CART-Based Classification and Forecasting Model Framework

The Classification and Regression Tree (CART) method introduces a data-driven approach to segmenting the training dataset. Unlike the Rule-Based classification, which relies on predefined calendar rules, the CART classification model automatically identifies optimal splitting thresholds based on the predictor variables, Month of Year (MoY), Day of Week (DoW), Holiday, and Bridging Holiday. Through recursive binary partitioning, the CART algorithm divides the dataset into leaf nodes, where each node represents a subset of days with similar load behaviors. Separate forecasting models are trained at each leaf node using only the data belonging to that node. During testing, each test day is assigned to a corresponding leaf node, and its forecast is generated using the model trained on that node's data.

3.2.4 Random Forest Classification

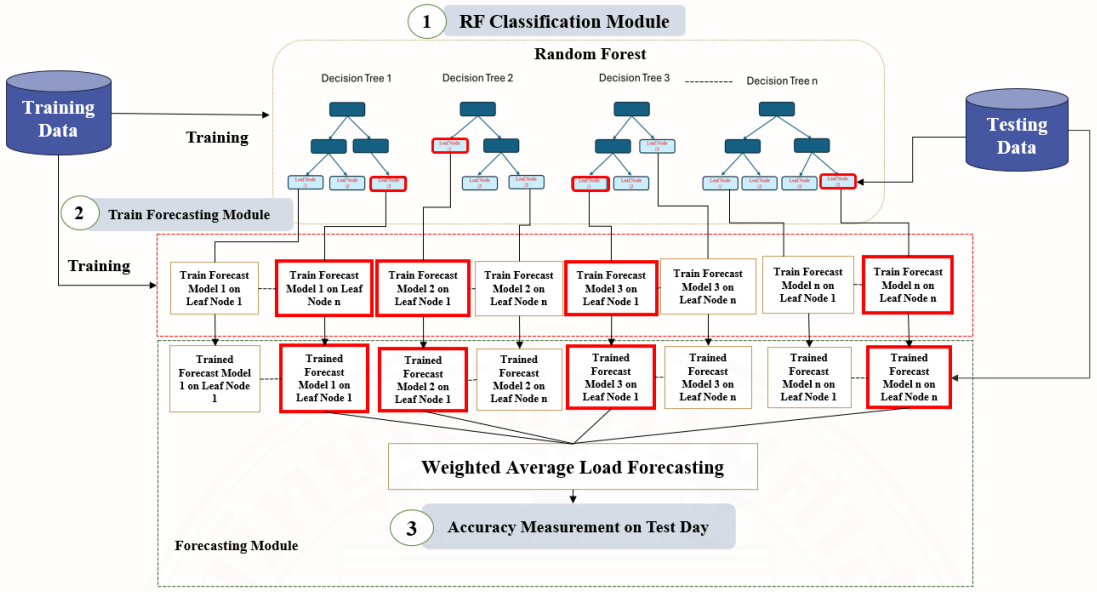

Figure 3.3 Random Forest Classification and Forecasting Framework

The Random Forest Classification represents the most advanced approach used in this study and forms the foundation of the proposed hybrid forecasting model. RF is an ensemble of multiple decision trees, each trained using randomly selected subsets of the training data and input features, including Month of Year (MoY), Day of Week (DoW), Holidays (Hol), and Bridging Holidays (B-Hol). For each test day, the model determines the leaf node in each tree where it falls, and the corresponding subset of training data in that leaf is used to train an individual forecasting model.

3.2.5 Node Splitting in Tree-Based Methods

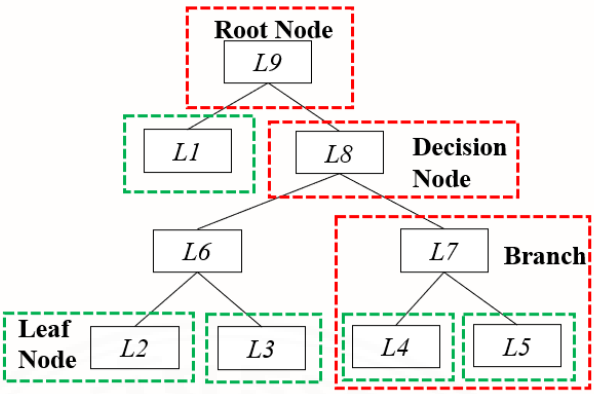

Figure 3.4 Structure of a Decision Tree

Figure 3.4 illustrates how the Decision Tree splits the training data based on classification features. The tree starts from the root node, divides samples at decision nodes, and ends at leaf nodes (l_1, l_2, l_3) containing similar load patterns. Each leaf node represents a group of days with comparable characteristics and serves as the training subset for forecasting models.

Table 3.1 Sample of Training Data for Tree-Based Classification.

No.	Type	Date	Independent Variables for Classification (Features)				Target Variable (Peak Load)
			MoY	DoW	Hol	B_Hol	L_{t1}
1	Train	14-10-19	10	1	1	0	18832.4
2	Train	15-10-19	10	2	0	0	19546.8
3	Train	16-10-19	10	3	0	0	22190.8
4	Train	17-10-19	10	4	0	0	22817.2
5	Train	18-10-19	10	5	0	0	22601.3
6	Train	19-10-19	10	6	0	0	22395.6
7	Train	20-10-19	10	7	0	0	22142.6
8	Train	21-10-19	10	1	0	0	20544.0
9	Train	22-10-19	10	2	0	0	22737.9

In the Tree-Based Classification model, the splitting process is guided by the Mean Squared Error (MSE) at each node, resulting in training sample groups with homogeneous load characteristics. At each decision node, the algorithm evaluates potential splits across all available independent features. It calculates the resulting MSE for each possible split calculates the resulting MSE for each possible division.

$$MSE_{split} = \frac{S_n^{left}}{S_n^{total}} MSE_{left} + \frac{S_n^{Right}}{S_n^{total}} MSE_{right} \quad (3.1)$$

The feature and threshold that minimize the post-split MSE are selected as the optimal partitioning criterion. This ensures that each subsequent data subset, as well as each child node, contains samples with similar calendar attributes and load patterns, thereby reducing variability and improving model interpretability.

In Random Forest (RF) Classification, this process is further enhanced by random feature selection, which, together, improves generalization and reduces overfitting. Instead of evaluating all input features at every split, the Random Forest algorithm randomly selects a subset of features for each tree, commonly defined by the parameter max-features = sqrt. This randomness ensures that individual trees capture different aspects of the calendar-load relationship, promoting diversity within the ensemble. Each tree in the forest independently identifies the feature splits that minimize its node-level MSE, producing multiple classification trees that collectively form a robust ensemble model.

Step 1*: Computing Root Node MSE*

In the first step of tree construction, all training samples are centralized into a single root node. The CART algorithm evaluates the heterogeneity of this node using the Mean Squared Error (MSE), which measures the variation of target load values around the mean of the node. This MSE acts as a baseline for impurity that will be reduced through subsequent splits. A high MSE suggests that the node contains samples with diverse load characteristics, indicating that data partitioning will improve homogeneity and, consequently, enhance the reliability of subsequent forecasting steps.

$$Number\ of\ samples\ in\ node\ n = s_n = 9 \quad (3.2)$$

$$Average\ Load\ in\ Node\ n = L_{avg}^{n} = \frac{\sum_{d=1}^{n} L_{t=1}^{d}}{s_n} = \frac{193{,}808.6}{9} = 21{,}534.28 \quad (3.3)$$

$$MSE_{Root} = \frac{1}{s_9}\sum_{d=1}^{9}\left(L_{t=1}^{d} - L_{avg}^{9}\right)^2 = \frac{18{,}006{,}947.15}{9} = 2{,}000{,}771.9 \quad (3.4)$$

Step 2: *Identifying Candidate Split Features*

After assessing the impurity of the root node, the algorithm examines each feature in the dataset as a potential splitting variable. For categorical calendar indicators such as Holiday and Bridging Holiday, binary splits are considered, whereas ordinal features such as Day of Week and Holiday are evaluated using meaningful threshold values. At this stage, all potential splits remain candidates, so the algorithm enumerates the feasible splits that could lead to a more homogeneous data group in subsequent steps.

Step 3: *Computing MSE for Decision Node*

For each candidate feature, CART simulates a split and measures the resulting reduction in impurity. The data are divided into left- and right-child nodes based on the feature threshold, and the MSE for each child node is calculated. The weighted post-split MSE is then obtained by combining the impurities of the child nodes in proportion to their weights. This step quantifies how effectively each feature partitions the data into subsets with reduced load variability, forming the basis for selecting the optimal split.

For Holiday,

$$Number\ of\ samples\ in\ node\ n = s_n = 1 \quad (3.5)$$

$$Average\ Load\ in\ Node\ n = L_{avg}^{n} = \frac{\sum_{d=1}^{n} L_{t=1}^{d}}{s_n} = \frac{18{,}832.4}{1} = 18{,}832.4 \quad (3.6)$$

$$MSE_{Hol} = \frac{1}{s_1}\sum_{d=1}^{1}\left(L_{t=1}^{d} - L_{avg}^{1}\right)^2 = \frac{0}{1} = 0 \quad (3.7)$$

For non-Holiday,

$$Number\ of\ samples\ in\ node\ n = s_n = 8 \tag{3.8}$$

$$Average\ Load\ in\ Node\ n = L^n_{avg} = \frac{\sum^n_{d=1} L^d_{t=1}}{s_n} = \frac{174{,}976.2}{8} = 21{,}872.02 \tag{3.9}$$

$$MSE_{\,non-Hol} = \frac{1}{s_8}\sum^8_{d=1}\left(L^d_{t=1} - L^1_{avg}\right)^2 = \frac{9{,}794{,}216.13}{9} = 1{,}224{,}277.26 \tag{3.10}$$

For Weekday,

$$Number\ of\ samples\ in\ node\ n = s_n = 7 \tag{3.11}$$

$$Average\ Load\ in\ Node\ n = L^n_{avg} = \frac{\sum^n_{d=1} L^d_{t=1}}{s_n} = \frac{149{,}270.4}{7} = 21{,}324.34 \tag{3.12}$$

$$MSE_{\,Weekday} = \frac{1}{s_7}\sum^7_{d=1}\left(L^d_{t=1} - L^7_{avg}\right)^2 = \frac{16{,}586.506.56}{7} = 2{,}369{,}500.93 \tag{3.13}$$

For Weekend,

$$Number\ of\ samples\ in\ node\ n = s_n = 2 \tag{3.14}$$

$$Average\ Load\ in\ Node\ n = L^n_{avg} = \frac{\sum^n_{d=1} L^d_{t=1}}{s_n} = \frac{44{,}538.2}{2} = 22{,}269.1 \tag{3.15}$$

$$MSE_{\,Root} = \frac{1}{s_2}\sum^2_{d=1}\left(L^d_{t=1} - L^7_{avg}\right)^2 = \frac{32{,}004.5}{9} = 16{,}002.25 \tag{3.16}$$

Step 4: *Evaluating and Comparing Impurity Reduction*

CART compares the weighted impurity values across all calendar features to determine which split yields the most significant improvement. A feature is considered more informative when it leads to child nodes with lower variability than the parent node. This comparison ensures that the selected split meaningfully enhances homogeneity in the training data, thereby improving the interpretability and predictive usefulness of downstream leaf nodes.

Step 5: *Selecting the Best Split for the Decision Node*

The feature associated with the lowest post-split impurity is selected as the optimal splitting rule for the decision node. This ensures that each dataset division maximizes the reduction in heterogeneity. The chosen feature becomes the decision

boundary at the node, and the dataset is partitioned accordingly. This step formally establishes the first layer of structure in the CART model and serves as the foundation for all subsequent splits.

$$MSE\ for\ split\ variable\ Hol = 1{,}088{,}246.459 \tag{3.17}$$

$$MSE\ for\ split\ variable\ DoW = 1{,}846{,}501.229 \tag{3.18}$$

Between the two candidate splits, the split using the Holiday (Hol) feature produces a lower weighted MSE than the split using the Day of Week (DoW) feature. In the CART algorithm, the criterion for selecting a split at each node is to choose the feature that yields the most significant reduction in impurity. A lower post-split MSE indicates that the resulting child nodes are more homogeneous and that the feature is more effective in separating days with similar load patterns. Since the MSE obtained from the Holiday split is smaller than the MSE obtained from the Day-of-Week split, the Holiday feature provides a clearer division of the data at this stage. For this reason, the Holiday split is chosen as the decision rule for the node, because it yields the most accurate and meaningful separation according to the CART splitting criterion.

Although the Holiday split produces a branch containing only a single holiday sample, this does not affect the splitting logic. A one-sample node naturally has zero impurity because there is no variation within the group, and it is treated as a terminal node without further partitioning.

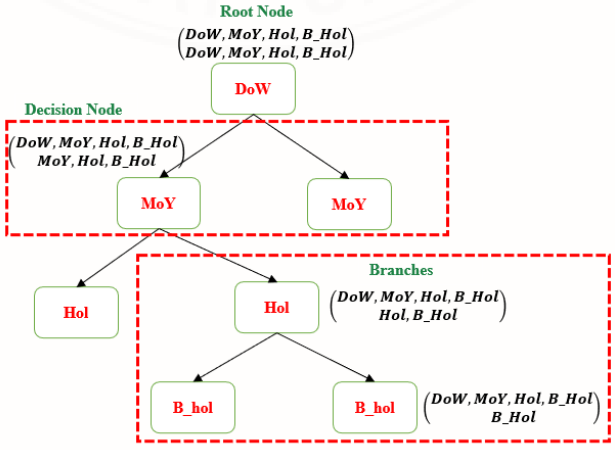

Figure 3.5 Example of Feature Splitting from the Root Node

Step 6: *Recursive Splitting of Child Nodes*

Following the first split, CART applies the same impurity-based evaluation process recursively to each child node. For each subset, the algorithm recalculates the node-level MSE, explores all potential splits on the remaining features, and measures the improvement in homogeneity. Through this recursive procedure, the decision tree grows branch by branch, progressively refining the grouping of days according to their calendar and load characteristics.

Step 7: *Evaluating Secondary Splits*

Within each child node, CART continues assessing candidate features in the same manner as at the root. Some features may no longer provide meaningful separation if the node contains limited or uniform values for that variable. Others may achieve substantial impurity reduction by distinguishing among different behavioral patterns within the remaining subset. At this stage, CART identifies which feature provides the most apparent differentiation in the context of the node's current composition.

Step 8: *Selecting the Best Split at Deeper Levels*

After computing impurity reductions for all secondary candidates, the algorithm selects the feature that produces the most homogeneous partitions. This ensures that the tree continues to grow in a direction that preserves interpretability and predictive quality. By consistently selecting the feature that minimizes impurity at each depth, CART constructs a hierarchical structure that mirrors the underlying relationships between calendar factors and electricity load behavior.

Step 9: *Constructing the Decision Path*

As splits accumulate through successive levels, a hierarchical decision structure forms. Each decision node corresponds to a feature threshold, and the path from the root to a given leaf node represents a sequence of calendar-based conditions defining a specific type of day. These decision paths group days with similar load characteristics, resulting in leaf nodes that contain the most behaviorally consistent subsets of the dataset.

Step 10: *Stopping the Splitting Process*

CART continues splitting nodes recursively until a stopping criterion is met, such as reaching a maximum tree depth, achieving minimal impurity reduction, or encountering nodes with insufficient sample size to justify further division. Once no further meaningful improvement is possible, the node is designated as a leaf. These leaf nodes then serve as the training subsets for the forecasting models, ensuring that predictions are based on groups of days sharing highly similar structural and behavioral attributes.

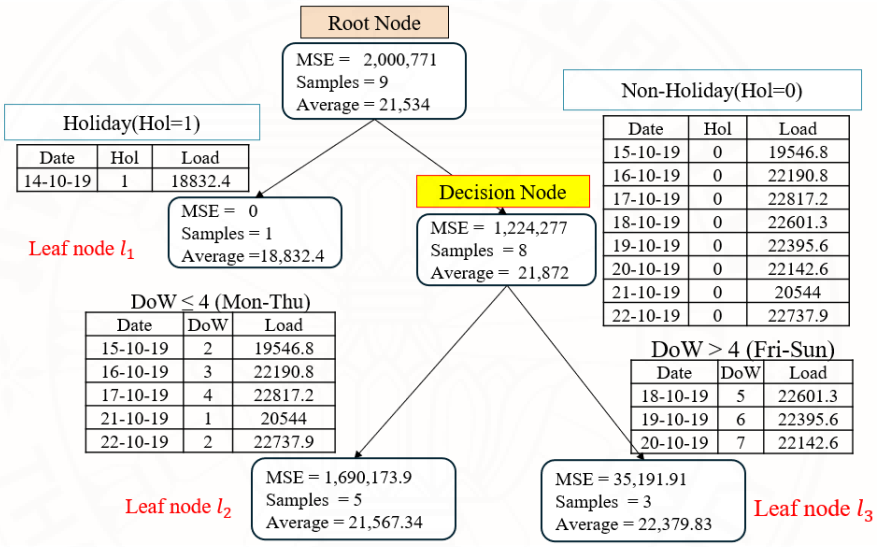

Figure 3.6 Illustration of Node Splitting in Tree-Based Classification

We tuned the Random Forest classifier's hyperparameter by sweeping the number of trees. $n_{estimators} \in \{1, \ldots, 100\}$ with fixed settings (criterion = squared error, max_features = $\sqrt{\cdot}$, max_depth = None, bootstrap = False). The best validation MAPE was obtained at $n_{estimators} = 10$, which is therefore used in all reported experiments.

Increasing forest size beyond 10 produced little to no reduction in MAPE and, in several cases, even slightly worsened it. In our two-stage design, each tree partitions days into fine-grained leaves, and the forecasting model is trained within the leaf to which the test day belongs. Adding too many trees increases segmentation granularity and can fragment the training data per leaf, leading to data sparsity and higher variance in downstream forecasts.

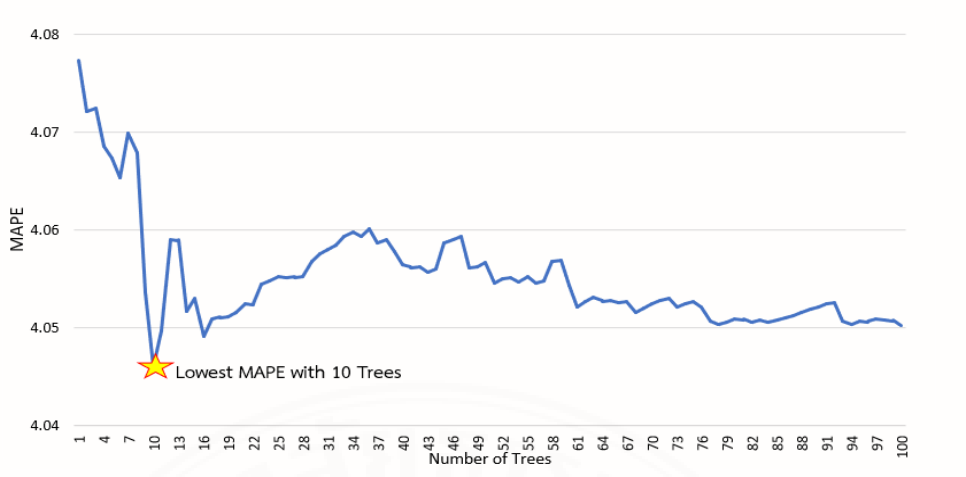

Figure 3.7 Effect of Number of Trees on RF Classification Accuracy

3.2.6 Feature Importance in CART and Random Forest Classification

Analysis of the importance of nature provides insight into how strongly each calendar attribute contributes to the tree-based models' classification decisions. In this study, feature importance for both CART and Random Forest classifiers is computed based on the total reduction in Mean Squared Error (MSE) attributed to each feature across all splitting nodes. The underlying principle corresponds to the splitting mechanism described earlier in Section 3.2.5, in which a feature is selected at each node if it yields the most significant reduction in impurity.

In the CART model, all available features are evaluated at each decision node, and the feature that yields the most significant reduction in MSE is selected. Because the root node split influences the most important proportion of the dataset, CART feature importance is highly sensitive to this initial decision. As a result, one dominant feature, typically the Month of the Year, receives disproportionately high importance. This behavior is consistent with the seasonal load variability illustrated earlier in Figures 1.2 and 1.3. Consequently, CART values tend to be less stable and more biased toward early splits.

In contrast, the Random Forest classifier introduces randomness by subsampling features at each node. Although all trees are trained on the same dataset, the random subset of candidate features forces different trees to consider alternative splitting variables. This promotes structural diversity among trees and reduces the dominance of any single feature. The final importance values, obtained by averaging

impurity reductions across all trees, provide a more balanced and generalizable estimate of each feature's predictive role.

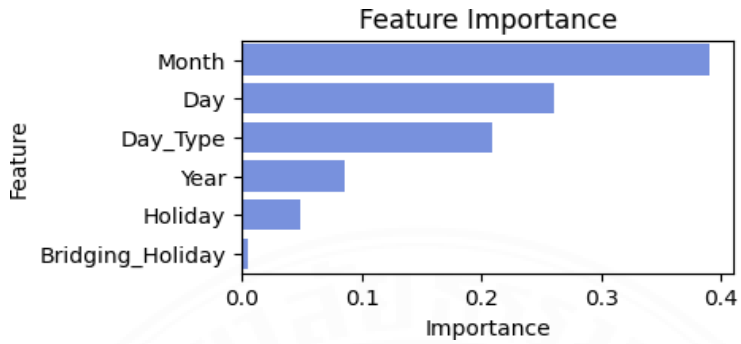

Figure 3.8 Feature Importance of Calendar Attributes in Tree-based Classifier

The resulting feature-importance ranking is presented in Figure 3.8, which shows that seasonal and weekly patterns are the strongest determinants of day-type classification. Meanwhile, holiday-related features exhibit much lower importance due to their infrequent occurrence and heterogeneous load behavior. These findings reinforce the rationale for using Random Forest classification as the foundation of the proposed hybrid forecasting framework.

3.3 Forecasting Models

The forecasting stage is performed after each classification module identifies the test day for its corresponding group. Three forecasting models, Multiple Linear Regression (MLR), Support Vector Regression (SVR), and Random Forest Regression (RF), are then used to estimate the load profile using five lagged inputs as independent variables, such as the load from the previous day, two days prior, three days prior, one week prior, and two weeks prior. In contrast, the target variable is the actual load of that day.

3.3.1 Multiple Linear Regression (MLR)

Multiple Linear Regression is a fundamental statistical method for modeling the relationship between a target variable and multiple independent variables. It assumes a linear relationship between the actual and the forecasted load.

$$F_t^g(d) = a_{0t}^g + a_{1t}^g L_t^g(d-14) + a_{2t}^g L_t^g(d-7) + a_{3t}^g L_t^g(d-3) + a_{4t}^g L_t^g(d-2) + a_{5t}^g L_t^g(d-1) \quad (3.19)$$

where $F_t^g(d)$ is forecasted load on day d at period t, $L_t^g(d-k)$ is actual load of the same period t on day $d-k$(with $k = 1,2,3,7,14$), a_{0t}^g is intercept term, $a_{1t}^g, a_{2t}^g, a_{3t}^g, a_{4t}^g, a_{5t}^g$ are regression coefficients representing the influence of past loads on the current forecasted load.

3.3.2 Support Vector Regression (SVR)

Support Vector Regression is a machine learning method derived from Support Vector Machines (SVM) that can capture both linear and nonlinear relationships between input features and target variables. SVR works by finding a regression function $f(x)$. That deviates from the actual data points by no more than a specified margin ϵ, while keeping the model as flat as possible.

For a given input feature vector:

$$x_g^t(d) = \left[L_t^g(d-1), L_t^g(d-2), L_t^g(d-3), L_t^g(d-7), L_t^g(d-14)\right]^T \quad (3.20)$$

$$F_t^g(d) = \sum_{i=1}^{N} (\alpha_i - \alpha_i^*)\, K\left(x_i^g, x_g^t(d)\right) + b \quad (3.21)$$

where N is number of support vectors, α_i, α_i^* is Lagrange multipliers (learned coefficients), $K(x_i^g, x_t^g(d))$ is kernel function measuring similarity between the training sample and the test input, b is bias term.

3.3.3 Random Forest Regression (RF)

Random Forest is an ensemble learning technique that combines multiple decision trees to produce a more accurate and stable prediction. Each decision tree in the forest is trained on a random subset of data and a random subset of features, introducing diversity among trees and reducing overfitting.

$$F_t^g(d) = \frac{1}{T}\sum_{n=1}^{T} F_{t,n}^g(d)\ \left(x_g^t(d)\right) x_g^t(d) \tag{3.22}$$

where T is total number of trees in the forest, $F_{t,n}^g(d)$ is the forecasted load from the n^{th}regression tree,

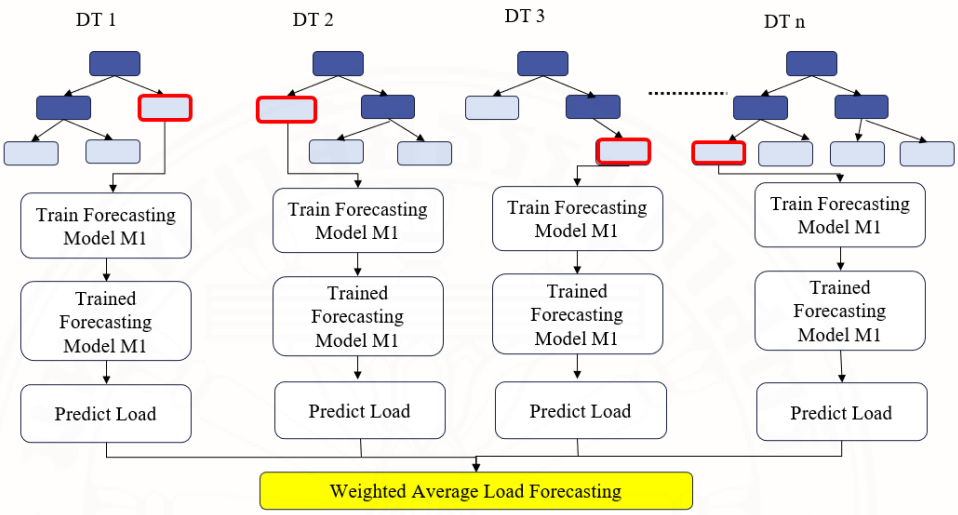

Figure 3.9 Averaging Predictions Across Trees in RF Regression

CHAPTER 4
DESIGN OF EXPERIMENTS

4.1 Dataset Description

The data we used in this study consist of two historical electricity load profiles for Thailand and France, obtained from EGAT and ENTSO-E, respectively, and both cover the three years from 2019 to 2021. The Thailand dataset comprises 48 half-hourly measurements per day, representing the net peak load recorded at 30-minute intervals, whereas French data contain 24 periods per day. Each record includes the date, time, day of week, month of year, holiday indicator, bridging-holiday indicator, and any additional notes identifying special calendar events.

The dataset captures a wide range of load behaviors influenced by seasonal weather patterns, weekday and weekend differences, and holiday structure. To ensure proper model evaluation, the data are divided chronologically: load profiles from 2019 to 2020 are used for model training, while 2021 serves as the testing year. This results in a training-to-testing ratio of approximately 67% to 33%, which is a standard practice in short-term load forecasting, where multi-year training data are required to capture seasonality and yearly trends.

France's electricity demand is strongly influenced by its temperate climate, with winter heating demand contributing to substantial load peaks, in contrast to Thailand's summer-driven peaks. The inclusion of France enables cross-country comparison, allowing the proposed methodology to be assessed under two distinct climatic and behavioral load regimes. Together, the Thai and French datasets provide complementary perspectives for evaluating the robustness and generalizability of calendar-aware classification and forecasting models, offering insights into how climatic and cultural differences shape short-term load patterns.

4.2 Data Preprocessing

Before model development, the raw load data are cleaned to ensure temporal consistency and analytical readiness. Basic preprocessing steps are applied to address missing entries and minor reporting irregularities. In addition, calendar features were

constructed for both Thailand and France to capture systematic variations in electricity demand. For both countries, day-type labels were assigned using official public holiday announcements, with bridging holidays identified when a day fell between a weekend and a public holiday or between two consecutive holidays. Remaining days were categorized as weekdays or weekends.

This preprocessing stage ensured that the dataset was complete, chronologically aligned, and equipped with accurate calendar-event information for subsequent classification and forecasting.

4.3 Data Arrangement for Classification Approaches

Table 4.1 presents the structure of the training and testing datasets used in the tree-based classification models. The classification stage relies exclusively on calendar features to group days with similar load characteristics before applying forecasting models. Four input features are used: Day of Week (DoW), Month of Year (MoY), Holiday (Hol), and Bridging Holiday (B-Hol). These features capture the calendar-driven behavior of electricity consumption, where DoW represents weekday-weekend effects, MoY reflects seasonal demand changes, Hol identifies official public holidays with irregular load patterns, and B-Hol distinguishes transitional days that fall between holidays and weekends. The target variable for classification is the day index $F_t^g(d)$, which assigns each date to a specific leaf or class generated by the tree-based algorithm.

Table 4.1 Train and Test Data Partition for Tree-Based Classification

	No.	Input Variables for Classification				Target Variable
		DoW	MoY	Hol	B_Hol	$F_t^g(d)$
Training Dataset	1	2	1	1	0	2019/01/01 (Tues)
	2	3	1	0	0	2019/01/02 (Wed)
	.	.	.	.	.	.
	.	.	.	.	.	.
	731	4	12	1	0	2020/12/31 (Thu)
Testing Dataset	1	5	1	1	0	2021/01/01 (Fri)

4.4 Data Arrangement for Forecasting Models

The forecasting stage uses a consistent regression structure based on five lagged load variables: $L_t^g(d-14)$, $L_t^g(d-7)$, $L_t^g(d-3)$, $L_t^g(d-2)$, and $L_t^g(d-1)$ representing the load values from two weeks, one week, three days, two days, and one day before the predicted day. The target variable $F_t^g(d)$is the actual load of the test day. Although the regression inputs remain the same across all forecasting methods, the arrangement of training samples differs depending on the classification scheme used in Stage 1. The following subsections explain how forecasting data were selected under each classification method.

Table 4.2 Data Arrangement of Forecasting Models with Everyday Classification Approach

	No.	Input Variables for Regression					Target Variable
		$L_t^g(d-14)$	$L_t^g(d-7)$	$L_t^g(d-3)$	$L_t^g(d-2)$	$L_t^g(d-1)$	$F_t^g(d)$
Training Dataset	1	2020/12/03 (Thurs)	2020/12/10 (Thurs)	2020/12/14 (Mon)	2020/12/15 (Tues)	2020/12/16 (Wed)	2020/12/17 (Thurs)
	2	2020/12/04 (Fri)	2020/12/11 (Fri)	2020/12/15 (Tues)	2020/12/16 (Wed)	2020/12/17 (Thurs)	2020/12/18 (Fri)
	.	.	.	.	.	.	.
	.	.	.	.	.	.	.
	20	2020/10/22 (Tues)	2020/12/29 (Tues)	2020/01/02 (Sat)	2020/01/03 (Sun)	2020/01/04 (Mon)	2020/01/05 (Tues)
Testing Dataset	1	2020/10/23 (Wed)	2020/12/30 (Wed)	2020/01/03 (Sun)	2020/01/04 (Mon)	2020/01/05 (Tue)	2021/01/06 (Wed)

Under the Everyday Classification approach, forecasting models do not distinguish between weekdays, weekends, holidays, or bridging holidays. All days are treated uniformly, and each forecasting model uses the twenty most recent previous days as the training set for each test day. This sliding-window strategy ensures that forecasting always relies on the latest load trends without considering calendar context. Table 4.2 shows that each training instance comprises the five lagged input variables and the corresponding load for the target day. The test day in 2021 is then predicted to use the relationship learned from the most recent twenty days in 2019 and 2020.

Table 4.3 Data Arrangement of Forecasting Models with Rule-Based Classification Approach

	No.	Input Variables for Regression					Target Variable
		$L_t^g(d-14)$	$L_t^g(d-7)$	$L_t^g(d-3)$	$L_t^g(d-2)$	$L_t^g(d-1)$	$F_t^g(d)$
Training Dataset	1	2020/10/14 (Wed)	2020/10/21 (Wed)	2020/10/25 (Sun)	2020/10/26 (Mon)	2020/10/27 (Tue)	2020/10/28 (Wed)
	2	2020/10/21 (Wed)	2020/10/28 (Wed)	2020/11/01 (Sun)	2020/11/02 (Mon)	2020/11/03 (Tue)	2020/11/04 (Wed)
	.	.	.	.	.	.	.
	.	.	.	.	.	.	.
	20	2020/12/16 (Wed)	2020/12/23 (Wed)	2020/12/27 (Sun)	2020/12/28 (Mon)	2020/12/29 (Tue)	2020/12/30 (Wed)
Testing Dataset	1	2020/10/23 (Wed)	2020/12/30 (Wed)	2020/01/03 (Sun)	2020/01/04 (Mon)	2020/01/05 (Tue)	2021/01/06 (Wed)

In the Rule-Based Classification approach, days are grouped into the categories of weekday, weekend, and holiday. Each forecasting model is trained on the twenty most recent historical samples of the same-day type as the test day. For example, to forecast a Wednesday in 2021, the model uses the previous twenty Wednesdays from the training period. This ensures that the regression model learns load behavior specific to each category, improving contextual consistency compared to Everyday Classification. Table 4.3 shows the data arrangement, in which all training rows share the same day type as the test sample. While this improves homogeneity, rare categories such as holidays and bridging holidays may have fewer available samples.

Table 4.4 Data Arrangement of Forecasting Models with Tree-Based Classification Approaches

	No.	Input Variables for Regression					Target Variable
		$L_t^g(d-14)$	$L_t^g(d-7)$	$L_t^g(d-3)$	$L_t^g(d-2)$	$L_t^g(d-1)$	$F_t^g(d)$
Training Dataset	1	2020/10/14 (Wed)	2020/10/21 (Wed)	2020/10/25 (Sun)	2020/10/26 (Mon)	2020/10/27 (Tue)	2020/10/28 (Wed)
	2	2020/10/21 (Wed)	2020/10/28 (Wed)	2020/11/01 (Sun)	2020/11/02 (Mon)	2020/11/03 (Tue)	2020/11/04 (Wed)
	.	.	.	.	.	.	.
	.	.	.	.	.	.	.
	n	2020/12/16 (Wed)	2020/12/23 (Wed)	2020/12/27 (Sun)	2020/12/28 (Mon)	2020/12/29 (Tue)	2020/12/30 (Wed)
Testing Dataset	1	2020/10/23 (Wed)	2020/12/30 (Wed)	2020/01/03 (Sun)	2020/01/04 (Mon)	2020/01/05 (Tue)	2021/01/06 (Wed)

For Tree-Based Classification methods, including CART and RF Classification, the assignment of training data is leaf-dependent rather than fixed. Each day is classified into a leaf node based on the combination of calendar features: Month of Year (MoY), Day of Week (DoW), Holiday indicator, and Bridging-Holiday indicator. After the classification step, the forecasting model for a test day uses only the historical samples that fall into the same leaf. As a result, the number of training samples is not constant; common combinations (e.g., mid-week working days) yield leaves with many samples, while rare combinations (e.g., holidays near weekends) produce leaves with fewer samples. Table 4.4 illustrates this dynamic structure, in which the set of training samples varies with the leaf assignment generated by the CART or RF classifier. This approach enhances segmentation precision but also necessitates fallback methods when leaf samples are insufficient**.**

4.5 Handling Insufficient Training Samples Using Naïve and Linear Interpolation Methods

When a test day's corresponding leaf has insufficient training data for model training, two fallback strategies, such as the Naïve Method and the Linear Interpolation

Method, are used to maintain data continuity and forecasting reliability. These methods are introduced to handle scenarios in which certain calendar types, such as rare holidays or unique bridging holiday combinations, have very few or no historical samples in the classification tree. This section explains (i) the naïve methods, (ii) their limitations, (iii) the proposed fallback strategy, and (iv) the holiday mapping and interpolation mechanism used in this study.

4.5.1 Naïve Method

The Naïve Method is a simple yet effective approach that assumes the load pattern of the most recent day is similar to that of the following day. In this study, if the test day was a typical day with insufficient training data, the Naïve approach used the load from the previous day $(d-1)$ as the proxy value for model training. This assumption is grounded in the short-term temporal stability of Thailand's daily load profiles, particularly in industrial and urban areas where electricity demand changes gradually from one day to the next. By referencing the previous day's actual load, the Naïve Method maintains short-term consumption continuity and prevents abrupt deviations in the model's learning.

The Naïve Method can be mathematically expressed as:

$$F_t^{T,l}(d) = \quad L_t^{T,l}(d-1) \tag{4.1}$$

Other naïve alternatives, such as using the previous week's load $L(d-7)$The last observed load within the leaf node was evaluated for comparison. However, they are not used as the primary benchmark for forecasting:

- $L(d-1)$ performs best overall and preserves short-term temporal behavior.
- $L(d-7)$ maintains weekday alignment but is unsuitable for holidays because last week is almost always a typical day.
- Leaf-node naïve load may come from a different month or holiday subtype due to RF's random feature splits (e.g., Month-of-Year), causing mismatched seasonal patterns even if both points are formally holidays.

Thus, $L(d-1)$ is adopted as the official naïve method for benchmark models.

Table 4.5 Performance Comparison of Naïve and Fallback Methods

Month	Naïve (Using L(d-7))		Naïve (Using L(d-1))		Naïve (Using leaf-node load $\boldsymbol{L_d^{T,l}}$)		Generalized Linear Interpolation		Fall Back Linear Interpolation using last year's holiday	
	MAPE	RMSE	MAPE	RMSE	MAPE	RMSE	MAPE	RMSE	MAPE	RMSE
January	62.37	61.65	13.66	13.79	12.53	12.68	38.02	37.22	13.89	14.40
February	6.41	7.18	4.75	5.67	7.91	8.36	11.12	11.61	4.09	4.83
March	-	-	-	-	-	-	-	-	-	-
April	25.31	26.16	4.64	5.66	7.06	7.56	14.73	15.33	10.79	12.28
May	8.04	8.87	9.81	11.22	14.53	15.05	4.33	5.17	6.96	8.09
June	8.61	9.42	7.88	9.69	43.09	43.75	5.43	6.43	8.61	9.42
July	10.27	11.28	10.80	11.80	8.88	9.66	11.88	12.55	7.86	8.92
August	10.44	12.47	13.76	15.37	7.18	7.78	3.76	4.90	5.26	5.83
September	1.39	1.92	1.46	1.70	5.13	6.43	3.93	4.76	2.09	2.39
October	4.71	5.92	6.01	7.13	5.29	5.49	3.40	4.40	4.01	4.63
November	-	-	-	-	-	-	-	-	-	-
December	20.72	21.49	11.12	11.68	6.30	7.25	21.66	21.89	4.12	4.82
Average	15.83	16.64	8.39	9.37	11.79	12.40	11.83	12.43	6.77	7.56

4.5.2 Limitations of Naïve Methods for Holidays and Bridging Holidays

Although $L(d-1)$ on typical days, naïve methods perform well. However, on holiday-related cases, they fail for several reasons. Holidays do not exhibit normal daily or weekly patterns, instead, their loads are shaped by cultural behavior, national travel flows, seasonal timing, and industrial shutdown schedules. Using either $L(d-1)$or $L(d-7)$often maps a holiday to a regular weekday, resulting in a significant mismatch. Furthermore, the RF leaf-node load may be misleading because leaf splits may occur based on Month-of-Year or other features, combining holidays from different seasons or contexts into the same leaf. This leads to poor estimates even if both samples are technically holidays.

Bridging holidays also cannot be handled by naïve assumptions because their behavior lies between a weekday and a holiday, requiring a blended, not direct, representation.

4.5.3 Fallback Linear Interpolation Method

To address the limitations above, the fallback Linear Interpolation Method uses a calendar-aware fallback mechanism that reflects the behavior of each day type.

(1) Normal days: If training samples are insufficient, the model uses the load from the same weekday of the previous week, $L(d-7)$. Weekly patterns remain stable for regular days, making this sound approximation.

$$F_t(d) = L(d-7) \tag{4.2}$$

(2) Holidays: For insufficient training samples, the model uses the load from the same holiday name in the previous year. Holiday-to-holiday repetition is high in Thailand, and last-year substitution yields much lower error than interpolation.

$$F_t(d) = L_{holiday}^{(same\ name, previous\ year)} \tag{4.3}$$

Table 4.6 Mapping of 2021 Thailand Public Holidays to Same-Name Holidays in 2020

2021 Date	Holiday Name	2020 Date (Same Holiday)
2021-01-01	New Year's Day	2020-01-01
2021-02-12	Chinese New Year	2020-01-25
2021-02-26	Makha Bucha Day	2020-02-10
2021-04-06	Chakri Day	2020-04-06
2021-04-12	Songkran Holiday	2020-04-13
2021-04-13	Songkran Day	2020-04-14
2021-04-14	Songkran Day	2020-04-15
2021-04-15	Songkran Day	2020-04-15
2021-05-03	Labour Day (sub.)	2020-05-01
2021-05-04	Coronation Day	2020-05-04
2021-05-10	Royal Ploughing Ceremony	2020-05-11
2021-05-26	Visakha Bucha Day	2020-05-06
2021-06-03	H.M. Queen Suthida's Birthday	2020-06-03
2021-07-25	Buddhist Lent	2020-07-06
2021-07-26	Asahna Bucha (obs.)	2020-07-07
2021-07-28	King's Birthday	2020-07-28
2021-08-12	Mother's Day	2020-08-12
2021-09-24	Prince Mahidol Day	2020-09-24
2021-10-13	King Rama IX Memorial Day	2020-10-13
2021-10-22	King Chulalongkorn (sub.)	2020-10-23
2021-12-05	Father's Day	2020-12-05
2021-12-06	King Bhumibol's Birthday	2020-12-07
2021-12-10	Constitution Day	2020-12-10
2021-12-31	New Year's Eve	2020-12-31

Table 4.7 Mapping of 2021 France Public Holidays to Same-Name Holidays in 2020

2021 Date	Holiday Name	2020 Date (Same Holiday)
2021-01-01	New Years's Day	2020-01-01
2021-04-05	Easter Monday	2020-04-13
2021-05-01	Labor Day	2020-05-01
2021-05-08	WWII Victory Day	2020-05-08
2021-05-13	Ascension Day	2020-05-21
2021-05-24	Whit Monday	2020-06-01
2021-07-14	Bastille Day	2020-07-14
2021-08-15	Assumption of Mary	2020-08-15
2021-11-01	All Saint's Day	2020-11-01
2021-11-11	Armistice Day	2020-11-11
2021-12-25	Christmas Day	2020-12-25

(3) Bridging holidays: These days reflect partial working activity and partial holiday behavior. Thus, the fallback uses a weighted linear interpolation between a weekday load and the nearest holiday load. This method estimates the missing load by taking a weighted average of the adjacent weekday and holiday loads. This produces a realistic intermediate value that reflects the partial working activity typically observed during such periods. Mathematically, if $L_t^{T,l}(d-7)$represents the weekday load and $L_t^{T,l}(d^*)\ is$ the holiday load, the forecasted bridging-holiday load $F_t^{T,l}(d)$was computed as:

$$F_t^{T,l}(d) = \quad \alpha\, L_t^{T,l}(d-7) + (1-\alpha) \quad L_t^{T,l}(d^*) \tag{4.4}$$

where $0 < \alpha < 1$ represents the relative influence of the weekday and holiday patterns.

CHAPTER 5
RESULTS AND DISCUSSION

5.1 Mean Absolute Percentage Error (MAPE)

MAPE measures the average percentage difference between the predicted and actual values. It shows how accurate your forecasting model is, expressed as a percentage**.**

$$MAPE^{g}(d)\ in\ \% = \frac{1}{N}\sum_{t=1}^{N}\left|\frac{L_t^g(d) - F_t^g(d)}{L_t^g(d)}\right| \times 100\% \quad (5.1)$$

where,

N = Number of periods

$L_t^g(d)$ = the actual load for group g at period t for day d,

$F_t^g(d)$ = the forecast load for group g at period for day d,

t = 1, 2, 3,,…,48 periods

5.2 Root Mean Square Error (RMSE)

RMSE measures the average magnitude of errors between predicted and actual values. It tells how much the predictions deviate, in the same units as the data.

$$RMSE^{g}(d)\ in\ \% = \frac{\sqrt{\frac{1}{N}\sum_{t=1}^{N}(\ \ L_t^g(d) - F_t^g(d))^2}}{\frac{1}{N}\sum_{t=1}^{N}\ \ L_t^g(d)} \times 100\% \quad (5.2)$$

where,

N = Number of periods

$L_t^g(d)$ = the actual load for group g at period t for day d,

$F_t^g(d)$ = the forecast load for group g at period for day d,

t = 1, 2, 3,…,48 periods

5.3 Monthly Forecasting Performance

The monthly evaluation of forecasting performance provides insights into how seasonal and calendar-driven variations affect short-term load-forecasting accuracy in Thailand and France. Tables 5.1 and 5.2 summarize the monthly Mean Absolute Percentage Error (MAPE) and Root Mean Square Error (RMSE) for Thailand, while Tables 5.3 and 5.4 report the corresponding results for France. In both cases, three forecasting models, such as Multiple Linear Regression (MLR), Support Vector Regression (SVR), and Random Forest (RF), are evaluated under five classification frameworks: Everyday, Rule-based, CART-based, Generalized RF-based, and the proposed RF classification.

Table 5.1 Monthly MAPE Comparison of Forecasting Models (Thailand)

Month	With Everyday Classification			With Rule-based Day Type Classification			With CART Day Type Classification			With RF Day Type Classification			The Proposed RF Classification		
	MLR	SVR	RF	MLR	SVR	RF	MLR	SVR	RF	MLR	SVR	RF	MLR	SVR	RF
Jan	8.62	11.30	9.66	5.99	14.95	10.02	11.24	14.72	11.48	6.67	10.20	6.75	8.69	12.35	8.73
Feb	4.86	6.40	5.10	3.14	4.02	3.91	4.10	5.66	4.39	4.43	5.93	4.68	4.00	5.26	4.14
Mar	3.18	6.03	3.70	2.94	13.57	4.89	3.02	3.27	2.71	3.56	3.48	2.85	3.56	3.48	2.93
Apr	8.41	11.73	9.16	5.47	9.81	5.88	9.66	7.09	5.68	8.28	6.52	5.53	9.96	6.11	5.06
May	6.70	7.62	7.21	5.62	9.82	5.27	5.76	5.77	4.82	6.96	6.71	5.75	6.43	5.33	4.44
Jun	4.98	5.37	5.40	3.06	5.53	5.72	4.97	6.06	4.96	4.61	4.92	4.15	4.28	4.39	3.60
Jul	4.85	6.47	5.29	4.52	6.04	4.62	5.64	4.71	4.32	6.21	5.33	5.13	8.83	4.40	3.72
Aug	5.78	5.53	6.88	4.45	4.88	4.42	4.27	4.38	4.13	5.13	4.80	4.41	4.27	3.80	3.29
Sep	3.66	3.93	3.85	2.83	4.69	3.06	3.72	3.38	3.08	3.11	2.86	2.46	3.43	2.93	2.54
Oct	5.07	5.51	5.30	2.98	3.25	3.30	4.44	3.55	3.55	4.20	3.90	3.65	4.35	3.55	3.12
Nov	4.41	5.09	4.59	2.22	4.00	3.21	3.04	3.75	3.04	2.73	3.78	2.78	2.86	3.81	2.88
Dec	8.76	9.02	7.97	6.40	12.01	7.94	8.92	7.65	7.10	4.78	5.48	4.65	4.26	4.68	4.06
Avg MAPE	5.77	7.00	6.18	4.14	7.71	5.19	5.73	5.83	4.94	5.06	5.33	4.40	5.41	5.01	4.03

Table 5.2 Monthly RMSE Comparison of Forecasting Models (Thailand)

Month	With Everyday Classification			With Rule-based Day Type Classification			With CART Day Type Classification			With RF Day Type Classification			The Proposed RF Classification		
	MLR	SVR	RF	MLR	SVR	RF	MLR	SVR	RF	MLR	SVR	RF	MLR	SVR	RF
Jan	9.75	11.82	11.88	6.98	14.55	9.87	8.83	12.18	8.97	8.17	11.35	7.63	10.53	12.63	9.10
Feb	5.54	7.00	6.04	3.68	4.04	3.90	3.42	5.02	3.73	5.64	6.85	5.46	5.10	5.76	4.57
Mar	3.77	6.52	4.49	3.38	13.61	4.90	3.03	3.27	2.71	4.41	3.78	3.27	4.37	3.76	3.32
Apr	9.76	12.32	11.53	6.73	10.59	6.60	8.07	5.82	4.93	10.83	7.69	6.73	14.99	6.88	5.87
May	7.59	8.39	8.89	6.63	9.94	5.33	4.97	4.97	4.00	8.42	7.56	6.74	8.48	5.96	5.09
Jun	5.81	6.13	6.70	3.40	5.44	5.59	4.24	5.36	4.25	5.64	5.49	4.86	5.27	4.97	4.19
Jul	5.55	7.17	6.38	5.92	6.73	5.30	5.27	4.40	4.02	7.62	6.35	6.07	9.06	5.02	4.34
Aug	6.63	6.31	8.40	4.93	4.69	4.23	3.79	3.96	3.68	6.34	5.76	5.38	5.16	4.39	3.87
Sep	4.20	4.57	4.68	3.46	4.71	3.08	2.91	2.58	2.28	3.92	3.48	2.99	4.25	3.48	2.98
Oct	5.98	6.16	6.62	3.61	3.25	3.31	4.43	3.55	3.56	5.34	4.65	4.41	5.75	4.08	3.66
Nov	5.03	5.72	5.76	2.68	4.01	3.22	2.95	3.61	2.89	3.54	4.30	3.24	3.61	4.22	3.26
Dec	9.53	9.62	9.58	7.31	11.80	7.83	7.23	6.11	5.59	5.75	6.07	5.32	5.19	5.11	4.56
Avg RMSE	6.59	7.64	7.58	4.89	7.78	5.26	4.93	5.07	4.58	6.30	6.11	5.18	6.81	5.52	4.47

Table 5.3 Monthly MAPE Comparison of Forecasting Models (France)

Month	With Everyday Classification			With Rule-based Day Type Classification			With CART Day Type Classification			With RF Day Type Classification			The Proposed RF Classification		
	MLR	SVR	RF	MLR	SVR	RF	MLR	SVR	RF	MLR	SVR	RF	MLR	SVR	RF
Jan	5.45	6.63	5.95	5.46	28.98	9.32	4.87	10.29	5.62	5.24	9.88	5.56	5.24	9.88	4.56
Feb	8.20	7.01	7.86	5.11	19.28	6.75	5.15	7.23	5.55	5.21	8.08	5.83	5.21	8.08	4.83
Mar	4.88	4.49	4.65	3.33	13.83	4.75	3.37	4.10	3.86	3.39	4.62	3.69	3.39	4.62	3.69
Apr	6.28	5.83	5.45	4.36	8.35	5.57	4.00	5.41	4.55	3.85	5.61	4.49	3.85	5.61	3.49
May	4.93	4.54	5.05	4.19	7.68	4.58	3.79	3.95	4.17	3.23	3.79	3.45	3.23	3.79	3.45
Jun	3.55	2.67	2.10	1.59	13.92	2.87	1.98	2.68	1.70	1.88	3.33	1.63	1.88	3.33	1.63
Jul	4.16	3.22	3.03	1.99	13.45	2.73	2.67	3.02	2.37	2.08	3.13	1.77	2.08	3.13	1.77
Aug	3.30	3.54	2.63	2.13	20.79	3.79	2.04	4.53	2.09	2.17	5.07	2.15	2.17	5.07	2.15
Sep	3.09	2.14	1.67	1.17	12.58	2.37	1.65	2.11	1.40	1.52	2.40	1.23	1.52	2.40	1.23
Oct	3.78	3.61	3.11	2.25	4.64	3.32	2.38	2.85	2.77	2.26	2.93	2.53	2.26	2.93	2.53
Nov	5.76	5.29	5.59	3.50	17.01	4.40	4.12	5.34	4.39	3.37	6.94	4.21	3.37	6.94	3.21
Dec	5.84	5.27	5.96	4.81	21.69	5.14	4.40	5.62	4.75	4.29	8.17	4.60	4.29	8.17	3.60
Avg MAPE	4.94	4.52	4.42	3.33	15.18	4.63	3.37	4.76	3.60	3.21	5.33	3.43	3.21	5.33	3.01

Table 5.4 Monthly RMSE Comparison of Forecasting Models (France)

Month	With Everyday Classification			With Rule-based Day Type Classification			With CART Day Type Classification			With RF Day Type Classification			The Proposed RF Classification		
	MLR	SVR	RF	MLR	SVR	RF	MLR	SVR	RF	MLR	SVR	RF	MLR	SVR	RF
Jan	6.71	8.75	7.83	6.89	29.97	11.26	6.51	13.42	6.98	7.00	12.48	6.90	7.00	12.48	6.90
Feb	9.68	9.17	9.85	6.47	23.91	9.67	6.65	10.74	7.24	6.72	11.30	7.62	6.72	11.30	7.62
Mar	5.93	5.56	5.90	4.26	15.53	5.74	4.25	5.04	4.89	4.32	5.56	4.64	4.32	5.56	4.64
Apr	7.87	7.37	7.22	6.53	10.27	7.01	5.61	6.79	6.31	5.29	7.44	6.24	5.29	7.44	6.24
May	6.44	6.06	6.62	5.73	8.92	5.51	5.16	5.32	5.62	4.34	4.97	4.50	4.34	4.97	4.50
Jun	4.88	3.47	2.77	2.00	14.39	3.73	2.57	3.21	2.21	2.40	4.24	2.11	2.40	4.24	2.11
Jul	5.62	4.49	4.59	2.72	14.23	3.45	4.04	4.18	3.92	2.93	4.15	2.51	2.93	4.15	2.51
Aug	4.49	4.27	3.34	2.86	21.80	5.29	2.64	5.63	2.82	2.82	6.32	2.86	2.82	6.32	2.86
Sep	4.42	2.88	2.18	1.46	12.86	2.95	2.22	2.61	1.95	2.02	3.10	1.67	2.02	3.10	1.67
Oct	4.93	4.41	4.09	2.93	5.49	4.32	3.05	3.45	3.57	2.96	3.64	3.24	2.96	3.64	3.24
Nov	7.19	6.96	7.25	4.62	19.23	5.46	5.32	6.56	5.75	4.49	9.63	5.69	4.49	9.63	5.69
Dec	7.09	6.29	7.36	6.10	24.19	6.33	5.37	6.84	6.03	5.33	10.13	5.85	5.33	10.13	5.85
Avg RMSE	6.27	5.81	5.75	4.38	16.73	5.89	4.45	6.15	4.77	4.22	6.91	4.49	4.22	6.91	4.49

5.3.1 Monthly MAPE Behavior

The monthly MAPE patterns closely follow the climatic and calendar characteristics of each country. For Thailand, higher MAPE values are observed in the hot season, especially April and May, which correspond to the peak summer period and include major holidays such as Songkran. During these months, rapid temperature increases, widespread air-conditioning use, and overlapping public holidays lead to sharp, irregular changes in load. Despite this, the proposed RF-RF model maintains low error levels, for example, around 5-6% in the most volatile months, clearly outperforming the Everyday and Rule-based approaches, which show much larger deviations. Elevated errors also appear in December and January, which coincide with Thailand's tourism season and New Year festivities. Load during this period is shaped by a combination of reduced industrial activity, increased travel, and higher residential and commercial usage in urban areas. Even under these conditions, the proposed model tracks the trend more accurately than competing methods.

In contrast, France exhibits a different seasonal error pattern that aligns with its temperate climate and heating-driven demand. Higher MAPE values tend to occur in winter and early spring (e.g., January, February, and occasionally November-December), when heating demand is high and sensitive to short-term temperature fluctuations. Rule-based SVR models show substantial errors in several winter months, reflecting their limited ability to adapt to complex interactions between temperature and calendar effects. The proposed RF-RF framework, however, significantly reduces these winter errors and achieves the lowest average MAPE throughout the year, around 3.0%, indicating strong robustness in handling heating-driven peak loads. During summer months, when French demand is lower and more stable, MAPE values drop further for all methods, but the RF-based approaches remain the most accurate.

Across both countries, Everyday and Rule-based classification strategies systematically yield higher MAPE. Everyday classification ignores day-type structure, while Rule-based classification relies on fixed, manually defined groups that can misrepresent irregular holidays or rare calendar combinations. CART-based segmentation improves performance by introducing data-driven splits, yet the single-tree structure may overfit or fail to capture all relevant seasonal regimes. RF-based classification and the proposed hybrid model, by aggregating multiple trees, learn a

more diverse and nuanced calendar, which explains their consistently lower monthly MAPE in both Thailand and France.

5.3.2 Monthly RMSE Behavior

The RMSE analysis complements the MAPE analysis by emphasizing the magnitude of significant prediction errors, particularly during peak-demand periods. In Thailand, the proposed RF-RF framework achieves the lowest average RMSE among all models, indicating that it effectively limits large residuals even during extreme conditions. As with MAPE, RMSE is slightly higher in April and May, when sudden temperature spikes and holiday effects drive strong demand surges, and in December and January, when tourism and festive activities alter standard load patterns. Nevertheless, the proposed RF-RF model consistently records lower RMSE than MLR and SVR models with Everyday, Rule-based, or single-tree CART classification. During the rainy season from June to October, when temperature and economic activity are more stable, RMSE values are typically in the 3-4% range, and the proposed model attains its best performance, reflecting its ability to exploit predictable calendar and seasonal structures.

For France, the RMSE results in Table 5.4 show a similar trend: the proposed RF-RF method delivers the most stable and lowest average RMSE across all months. Winter months, especially January, February, and December, naturally exhibit higher RMSE due to substantial, highly weather-sensitive heating loads. Rule-based SVR models often produce very large RMSE in these periods, indicating vulnerability to mis-specified day-type segmentation and sensitivity to outliers. In contrast, the RF models, particularly the proposed hybrid framework, smooth out such extremes by aggregating multiple calendar-aware trees, thereby improving generalization under rapidly changing winter conditions. In spring and summer, when French demand is lower and less volatile, RMSE values decrease for all methods. Still, the proposed RF-RF model maintains a clear advantage and demonstrates less month-to-month fluctuation than the CART-SVR combination.

Taken together, the monthly MAPE and RMSE analyses for both Thailand and France confirm that:

- Seasonal and calendar effects are critical: error peaks align with hot season cooling and festive periods in Thailand, and with winter heating in France.
- Simple temporal or rule-based classification is insufficient: Everyday and Rule-based strategies struggle in months with irregular holidays or strong weather sensitivity.
- Ensemble classification with RF is more robust: the proposed RF-RF framework consistently achieves the lowest or near-lowest errors across all months and both countries, demonstrating that a calendar-aware ensemble architecture generalizes well across contrasting climatic and load regimes.

5.4 Predicted vs. Actual Load Pattern Comparison

This section compares the predicted and actual load profiles generated by the proposed RF-RF framework for both Thailand and France across different day types. The prediction-curve figures highlight the model's ability to reproduce daily demand dynamics under diverse climatic, cultural, and operational conditions. Overall, the close alignment between the actual and estimated curves demonstrates that the model effectively captures short-term load behavior in two fundamentally different power systems.

5.4.1 Weekday Load Pattern

For weekdays, the predicted curves in both Thailand and France closely follow the actual load trajectories. In Thailand, the model accurately replicates the characteristic morning ramp-up, midday plateau, and evening stabilization typical of commercial and industrial activity. Minor deviations occur at midweek intervals, yet the error margins remain narrow, confirming that weekday load is highly regular and strongly dependent on work-hour demand patterns well learned from lagged features within the model.

France exhibits similarly strong weekday performance. Despite differences in climate and daily routines, such as more pronounced winter morning peaks driven by heating usage, the predicted curves maintain close correspondence with the observed profiles. The model successfully reproduces France's sharper weekday morning rise and evening secondary peak. Overall, the near-overlap of the two curves across most

weekdays indicates that the classification–forecasting pipeline generalizes effectively across regions with different demand drivers.

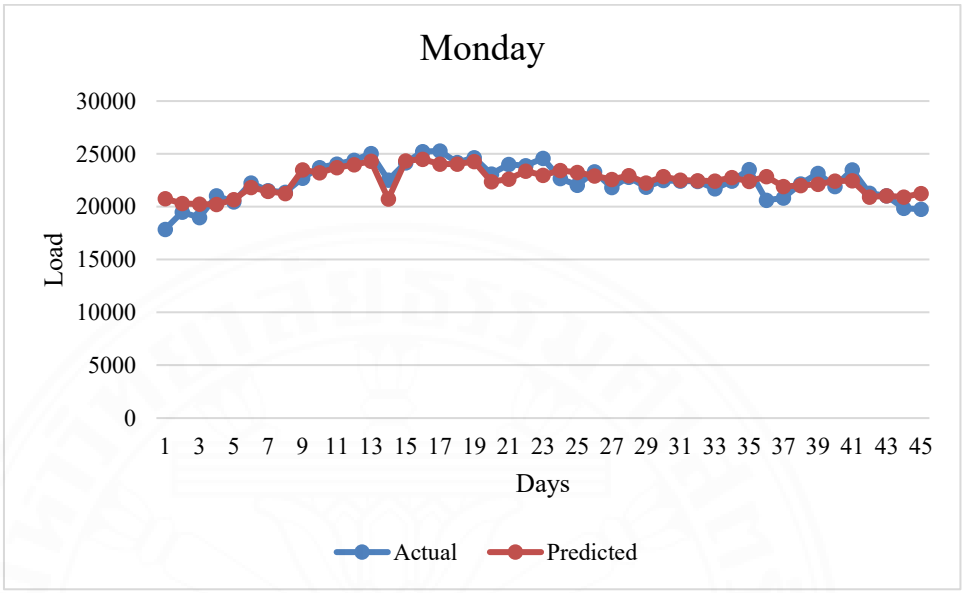

(i)

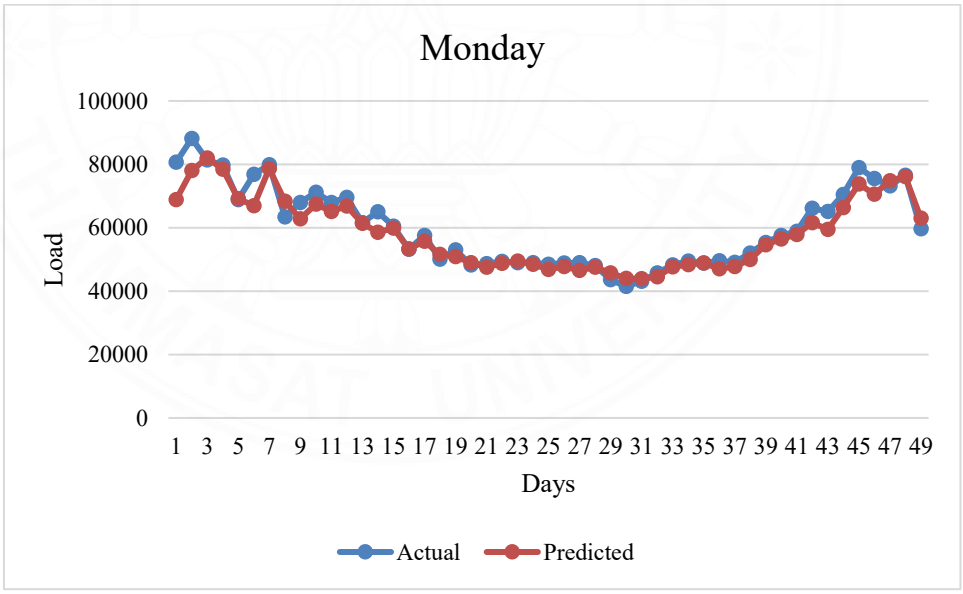

(ii)

Figure 5.1 Predicted vs Actual Monday Load Profile (i) Thailand and (ii) France

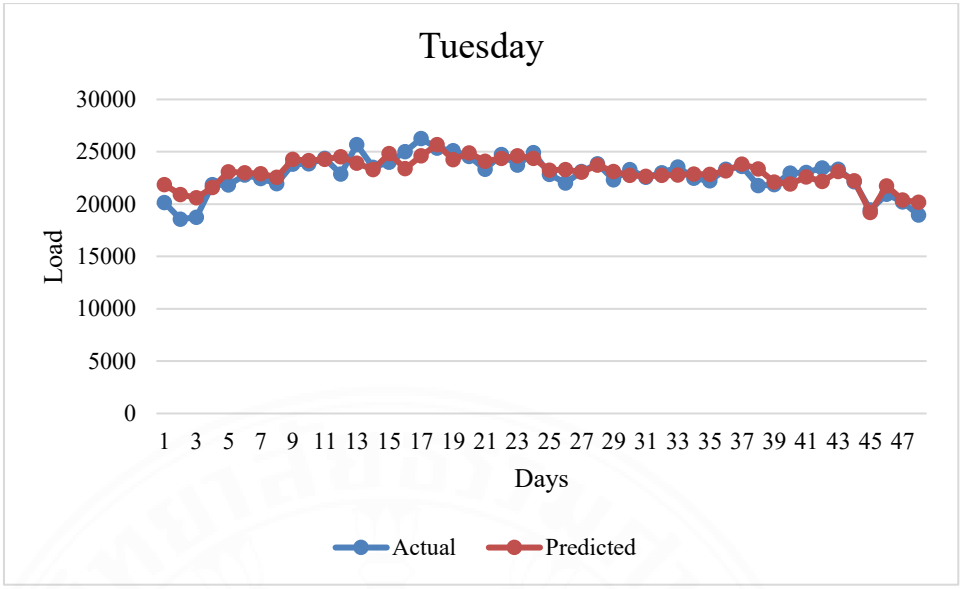

(i)

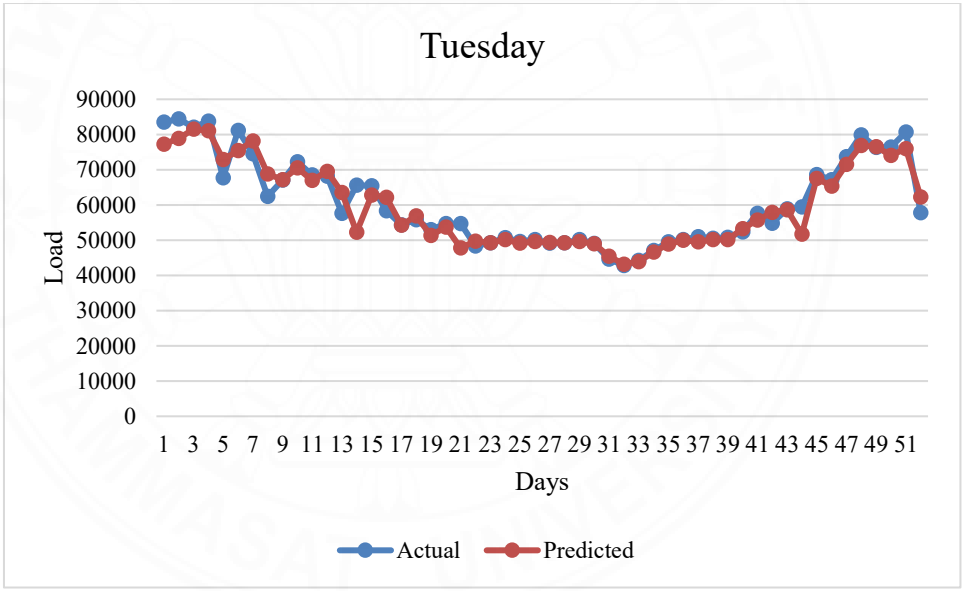

(ii)

Figure 5.2 Predicted vs Actual Tuesday Load Profile (i) Thailand and (ii) France

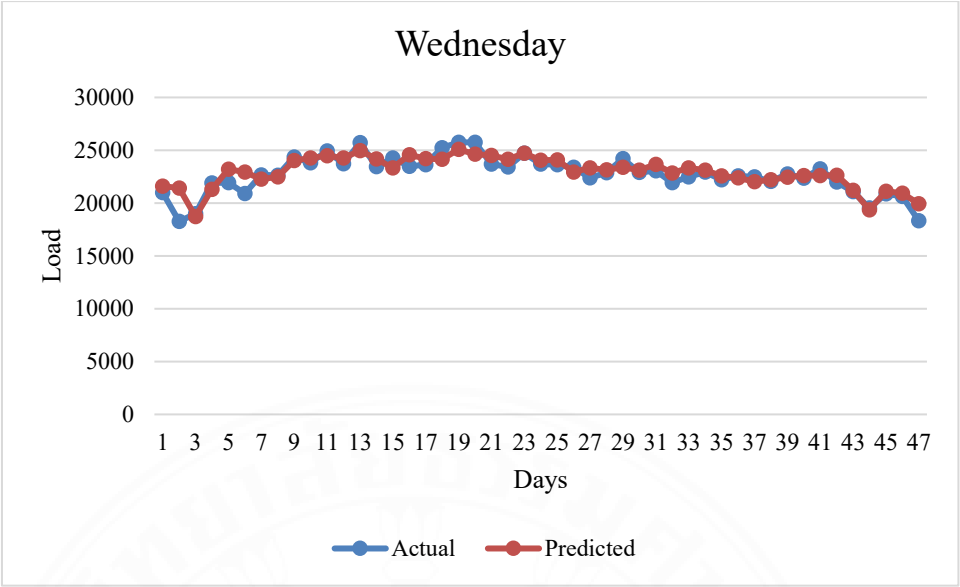

(i)

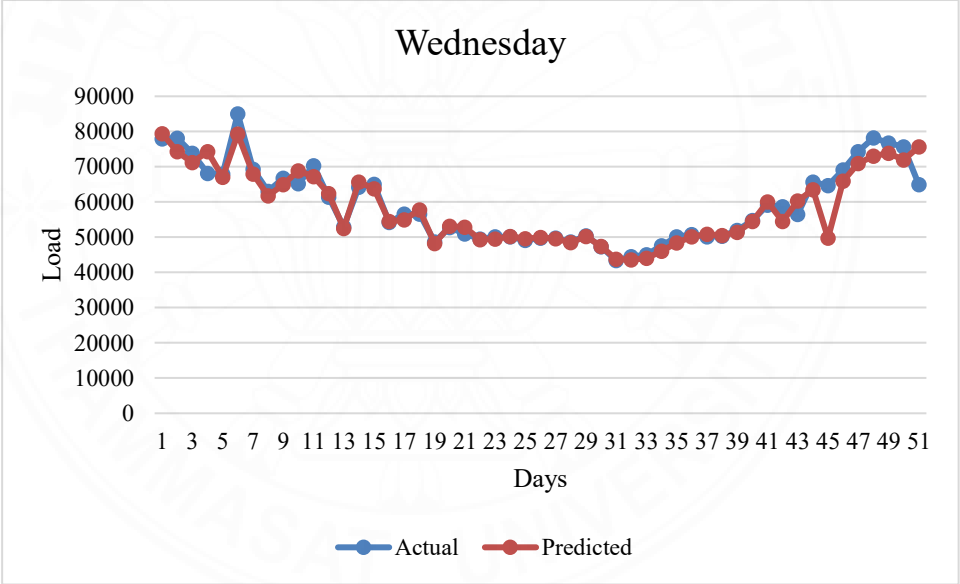

(ii)

Figure 5.3 Predicted vs Actual Wednesday Load Profile (i) Thailand and (ii) France

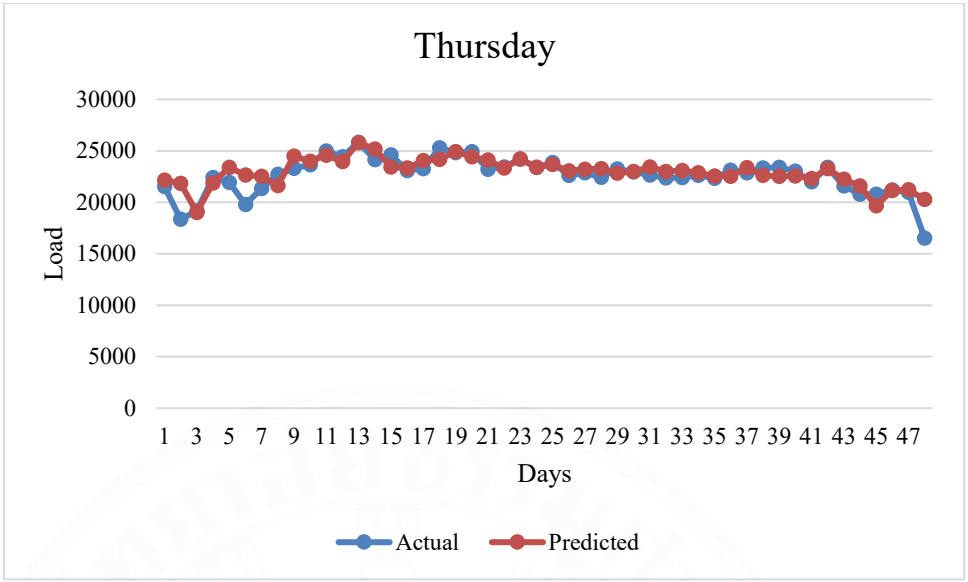

(i)

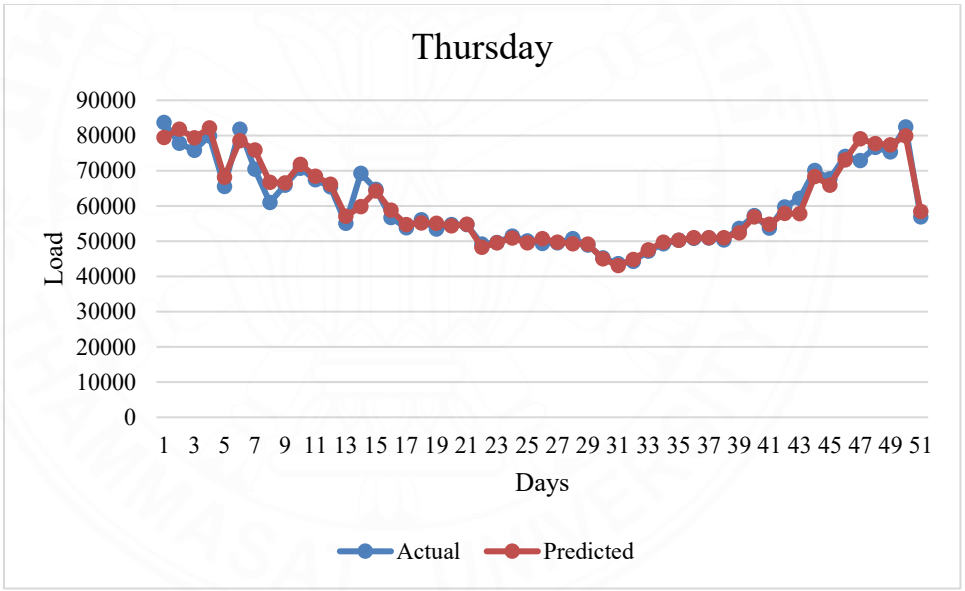

(ii)

Figure 5.4 Predicted vs Actual Thursday Load Profile (i) Thailand and (ii) France

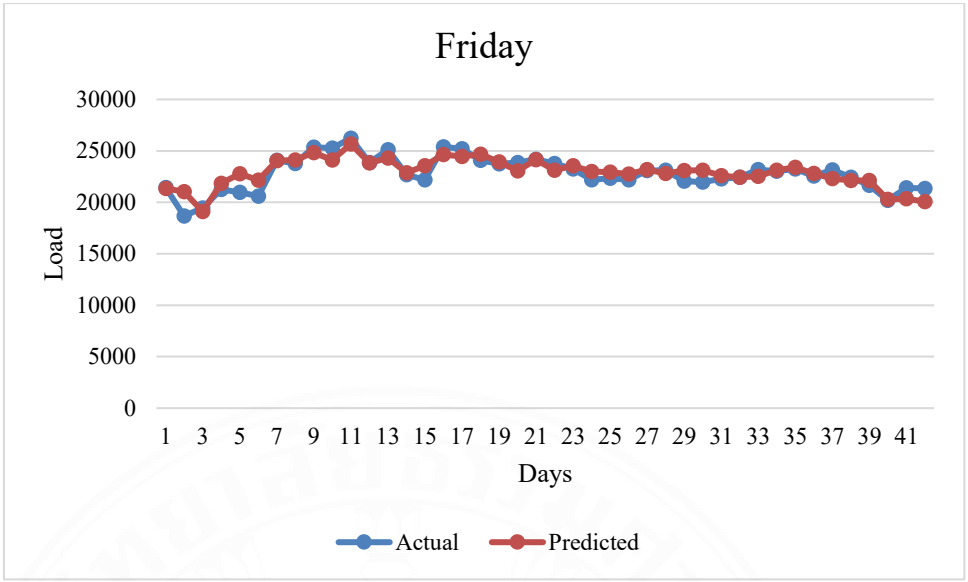

(i)

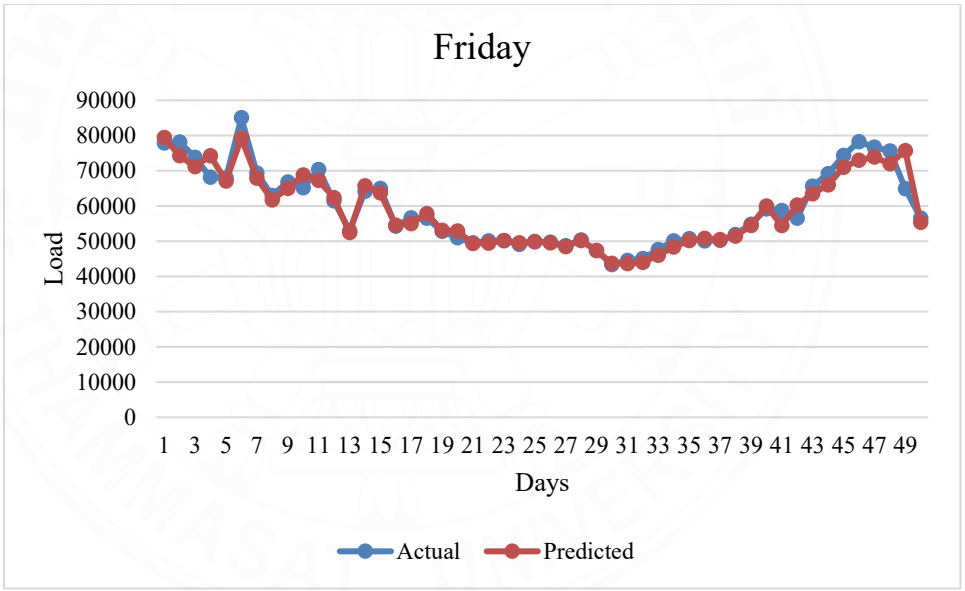

(ii)

Figure 5.5 Predicted vs Actual Friday Load Profile (i) Thailand and (ii) France

5.4.2 Weekend Load Pattern

Weekend behavior introduces greater variability in both countries due to reductions in industrial activity and more heterogeneous residential usage. In Thailand, the predicted series remains directionally consistent with the actual curve but exhibits slightly wider oscillations, reflecting the less-structured consumption typical of weekends. Similarly, in France, weekend profiles are flatter and more temperature-

dependent, yet the model still tracks primary turning points and maintains a stable error band. Despite these variations, the differences between actual and predicted values remain modest, indicating that Random Forest regression captures non-linear shifts in residential behavior without overfitting to weekday patterns.

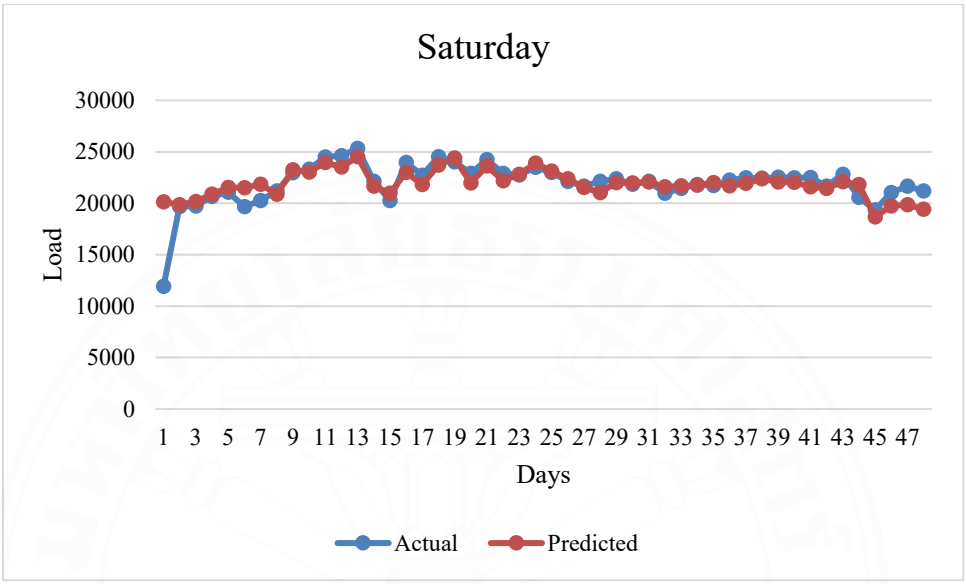

(i)

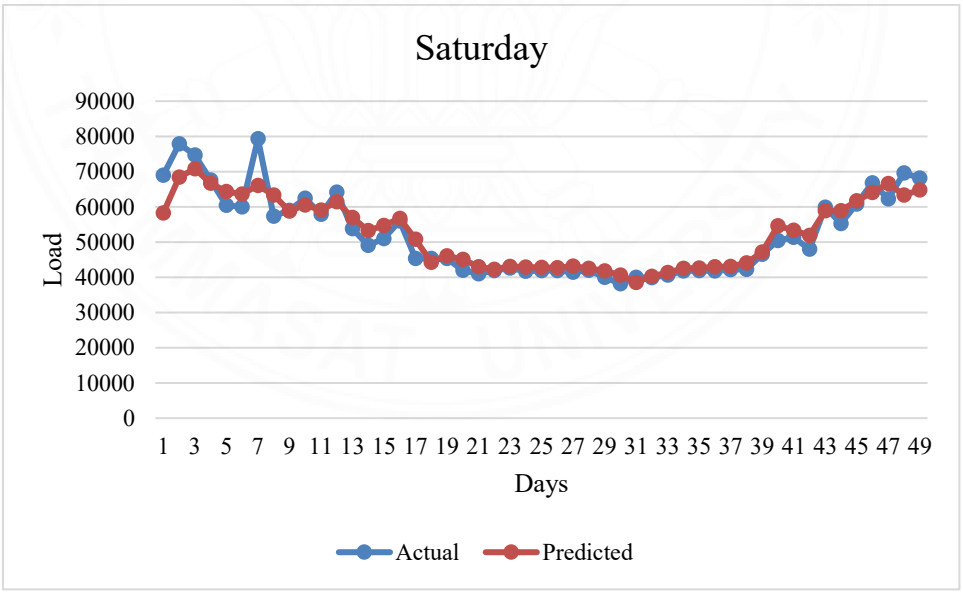

(ii)

Figure 5.6 Predicted vs Actual Saturday Load Profile (i) Thailand and (ii) France

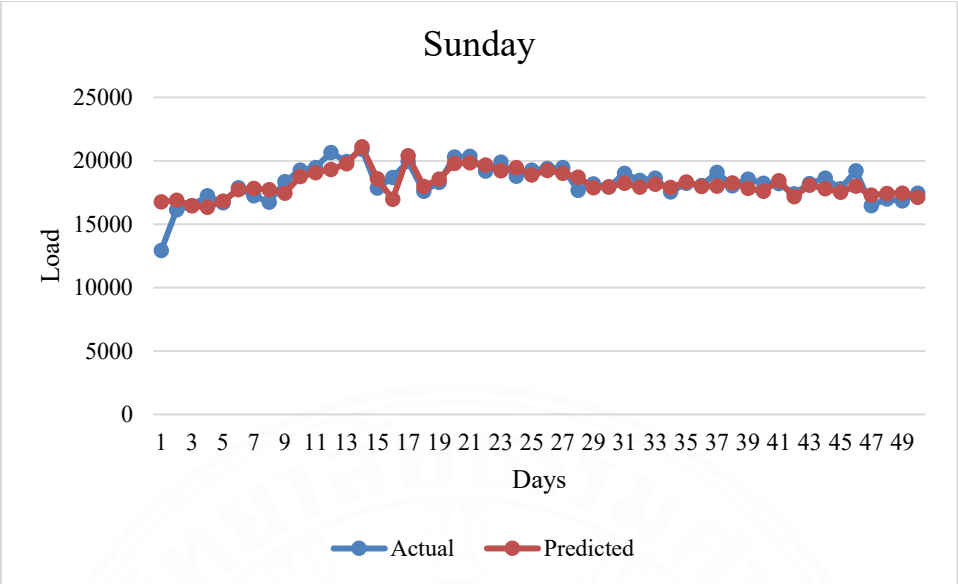

(i)

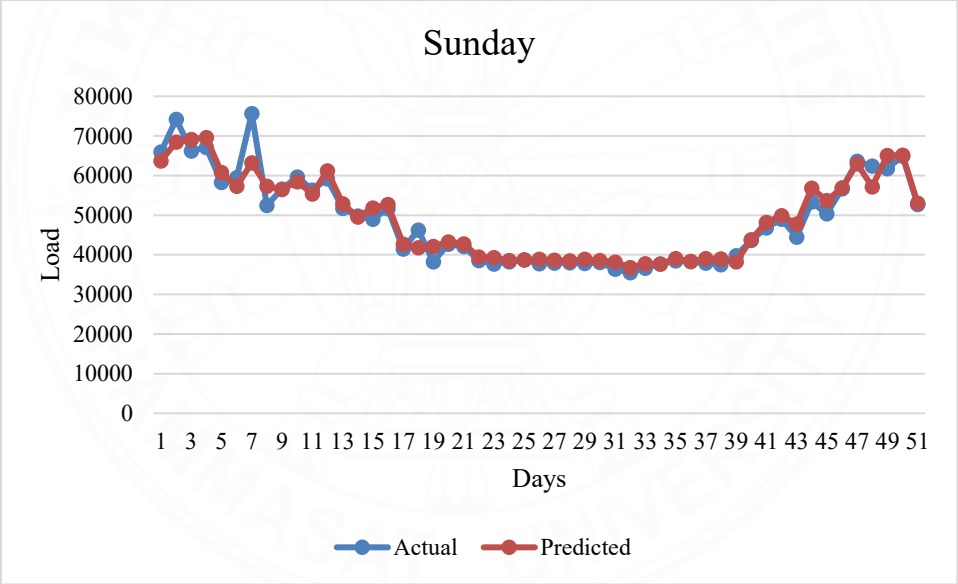

(ii)

Figure 5.7 Predicted vs Actual Sunday Load Profile (i) Thailand and (ii) France

5.4.3 Holiday Load Pattern

Forecasting accuracy decreases modestly during holidays because both Thailand and France experience irregular consumption influenced by travel, events, and reductions in commercial load. In Thailand, holiday curves often contain abrupt drops and post-celebration rebounds. The model follows these fluctuations but may

slightly overshoot during rapid declines due to the small number of holiday training samples.

In France, holidays similarly exhibit lower-than-normal load levels, but the pattern is shaped more by heating needs in winter or reduced activity in summer. Despite these structural differences, the predicted curves for both countries capture the overall shape and magnitude of holiday demand. The interpolation strategy applied for data-sparse leaf nodes ensures smoothness and prevents disruptive forecasting gaps.

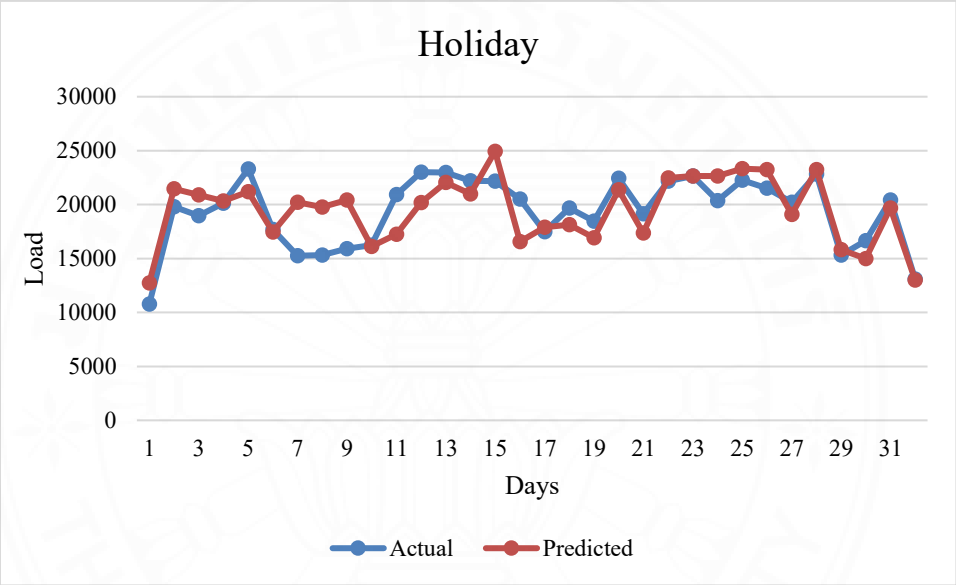

(i)

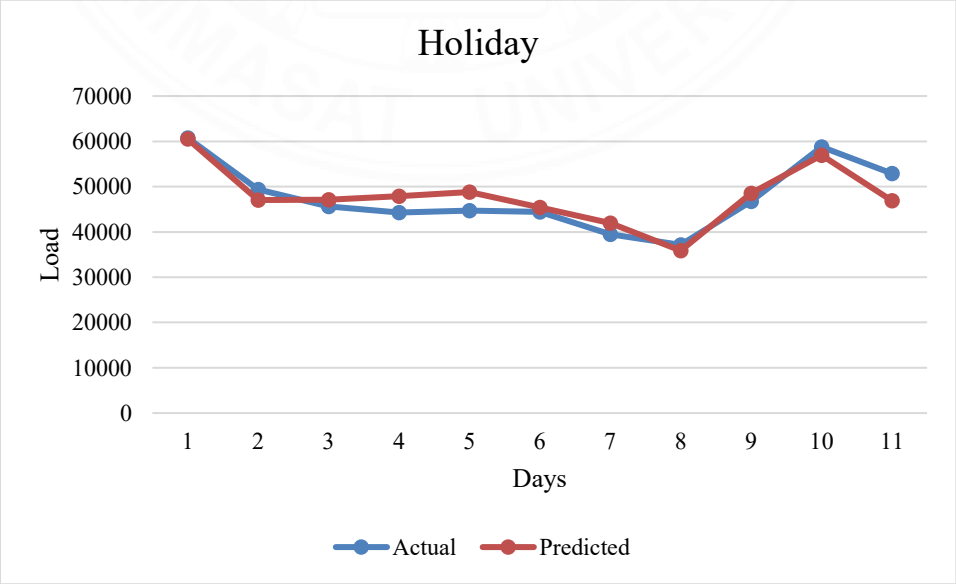

(ii)

Figure 5.8 Predicted vs Actual Holiday Load Profile (i) Thailand and (ii) France

5.4.4 Bridging Holiday Load Pattern

The bridging-holiday case in Figure 5.9 illustrates one of the most challenging forecasting scenarios. These transitional days display load levels between weekday and holiday behavior. The actual curve fluctuates sharply over a short time frame, yet the predicted series still tracks its overall direction and approximates its magnitude. The differences seen around the third day, where the actual load spikes more strongly than expected, highlight the hybrid nature of such days; even so, the model's adaptive interpolation effectively smooths the transition. This indicates that while complete accuracy for rare patterns remains difficult, the framework's two-stage design still provides reliable estimates for operational planning.

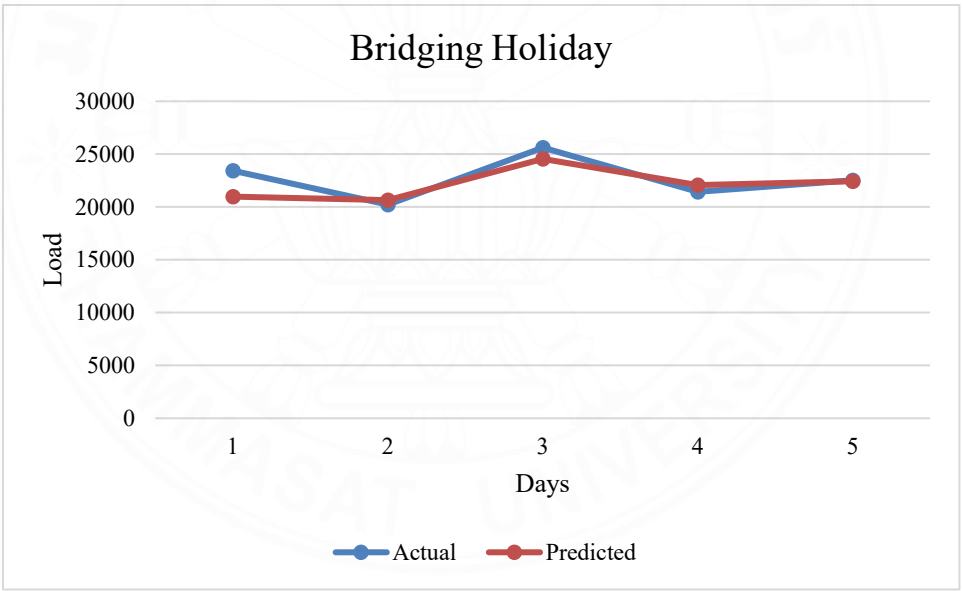

(i)

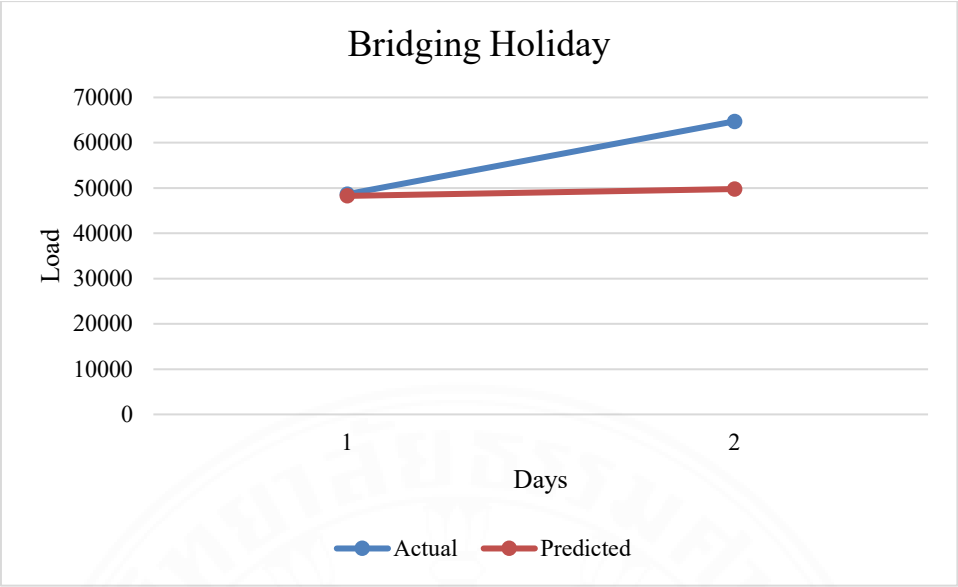

(i)

Figure 5.9 Predicted vs Actual Bridging Holiday Load Profile (i) Thailand and (ii) France

Overall, the comparison between actual and predicted curves across all nine figures demonstrates that the proposed hybrid Random Forest-classification and Random Forest-forecasting model can accurately predict actual load patterns. The close alignment of the curves, particularly on weekdays, confirms that the ensemble method captures both cyclical regularities and moderate irregularities in both datasets. Even under irregular conditions such as holidays and bridging holidays, the model preserves realistic trend behavior and avoids systematic bias. These results verify that the model's predictive performance is not only numerically strong but also visually consistent with real-world load dynamics.

5.5 Discussion in Relation to Thailand's Load Characteristics

The monthly forecasting performance reveals clear relationships between model accuracy and the underlying load characteristics of both Thailand and France. In Thailand, the variations in MAPE and RMSE correspond strongly to the country's climatic and socio-economic cycles. The summer months, from March to May, produce the highest national electricity demand due to intensive air-conditioning use, resulting in greater volatility and increased forecasting difficulty. The cool season from

November to February introduces additional uncertainty driven by tourism, extended festive periods, and irregular holiday schedules. By contrast, the rainy season from June to October exhibits the most stable load behavior, reflected in consistently low forecasting errors across all models. These findings confirm that Thailand's load profile is highly temperature-sensitive and strongly influenced by calendar events.

In France, a different pattern emerges, aligning with its temperate climate. The winter months from December to February generate the highest forecasting errors due to pronounced heating demand and strong morning and evening peaks. The transition seasons, spring from March to May and autumn from September to November, display moderate demand levels and more predictable load shapes, resulting in lower MAPE and RMSE values. Summer months in France exhibit the lowest overall errors, reflecting relatively stable load patterns and weaker cooling demand than in Thailand. These results demonstrate that, unlike Thailand's heat-driven consumption, France's load system is predominantly shaped by heating cycles and socio-economic rhythms tied to commuting and working hours.

Across both countries, the proposed calendar-aware Random Forest (RF) classification combined with RF forecasting delivers the most consistent performance. For Thailand, the hybrid approach achieves an annual average MAPE of 4.03% and RMSE of 4.57%, outperforming all baseline classification strategies. A similar trend is observed in France, where the proposed model achieves an MAPE of 3.31% and an RMSE of 3.85%, the lowest among all forecasting configurations.

Table 5.5 Overall Forecasting Performance under Different Classification Methods

Forecasting Models	Classification Approach	Thailand		France	
		MAPE (%)	RMSE (%)	MAPE (%)	RMSE (%)
MLR	Everyday	6.02	6.89	4.91	5.42
	Rule-Based	4.52	5.42	3.65	5.55
	CART	6.78	6.26	3.94	5.56
	RF	5.45	6.81	3.38	5.04
	Proposed	5.77	7.18	3.36	5.02
SVR	Everyday	7.25	7.85	4.52	5.81
	Rule-Based	7.78	7.99	15.18	16.73
	CART	5.31	4.96	4.76	6.14
	RF	5.55	6.46	5.19	6.00
	Proposed	4.97	5.50	5.31	6.15
RF	Everyday	6.47	7.90	4.42	5.75
	Rule-Based	5.57	5.78	4.63	5.89
	CART	4.38	4.58	3.59	4.21
	RF	4.71	5.60	3.37	3.90
	Proposed	4.03	4.47	3.31	3.85

Compared to simpler classification schemes, such as Everyday or Rule-Based grouping, the Random Forest-based classification demonstrates superior adaptability to atypical calendar patterns and climate-induced variability. While CART classification improves performance through feature-driven segmentation, its single-tree structure is inherently prone to overfitting, resulting in less stable monthly accuracy. In contrast, the proposed RF–RF framework leverages the diversity of multiple trees to develop more generalizable partitions and forecasts.

Overall, the monthly MAPE and RMSE results for Thailand and France underscore the robustness and cross-country applicability of the proposed method. The model consistently provides accurate forecasts across diverse climatic conditions, from Thailand's high-temperature seasonal peaks to France's winter-driven load cycles. These outcomes reinforce the value of integrating calendar-awareness with ensemble learning, offering a scalable and operationally practical forecasting solution for both tropical and temperate electricity systems.

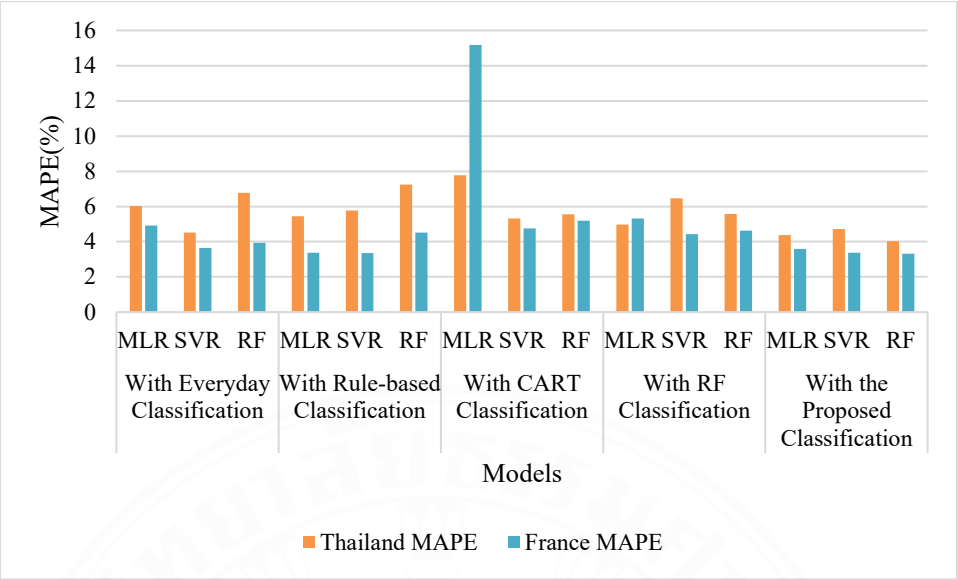

Figure 5.10 Average MAPE of Forecasting Models under Different Classification Methods

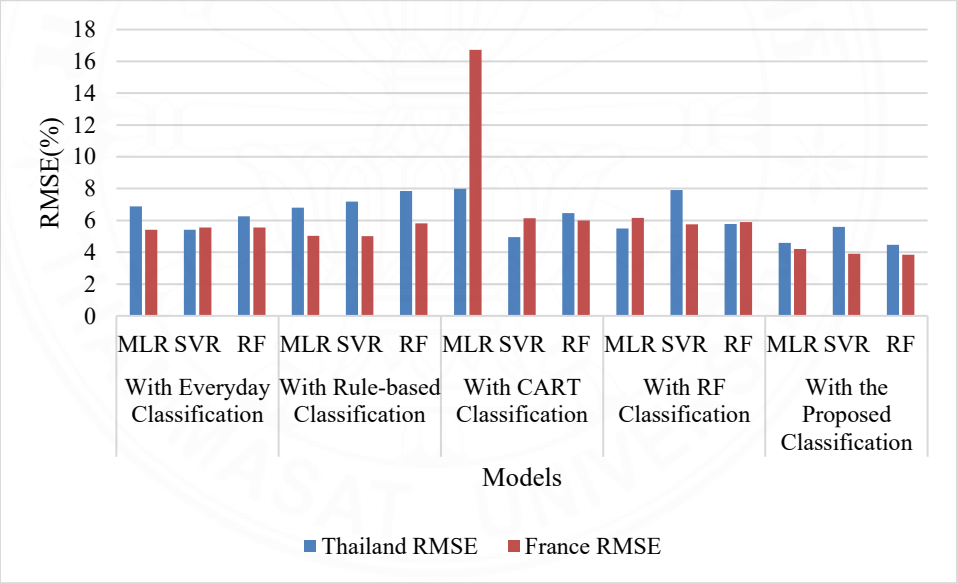

Figure 5.11 Average RMSE of Forecasting Models under Different Classification Methods

Figures 5.10 and 5.11 summarize the forecast performance of the proposed model and benchmark models. These figures provide a high-level understanding of how day-type variability and classification structure affect the accuracy of short-term load forecasting.

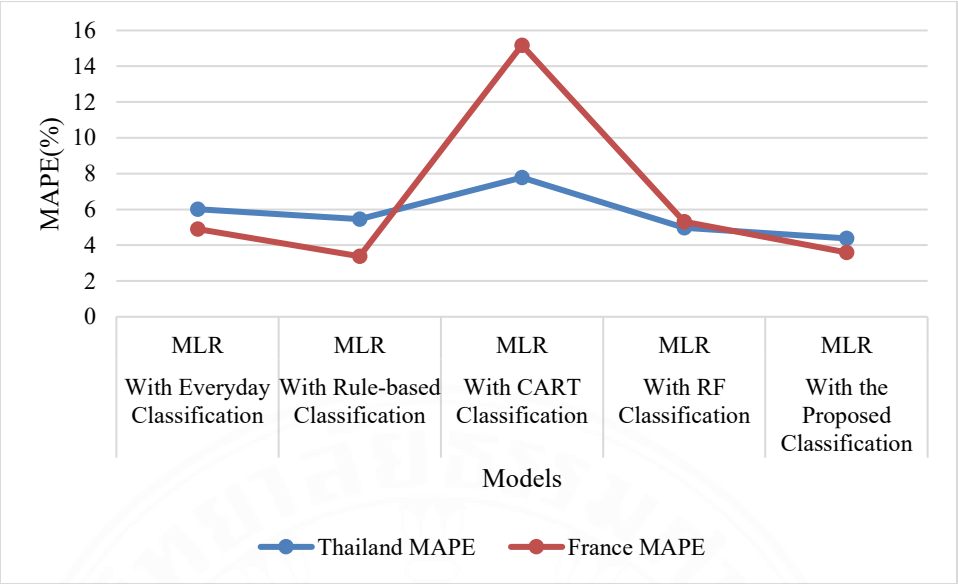

Figure 5.12 Cross-Country MAPE Comparison of MLR Forecasting Models

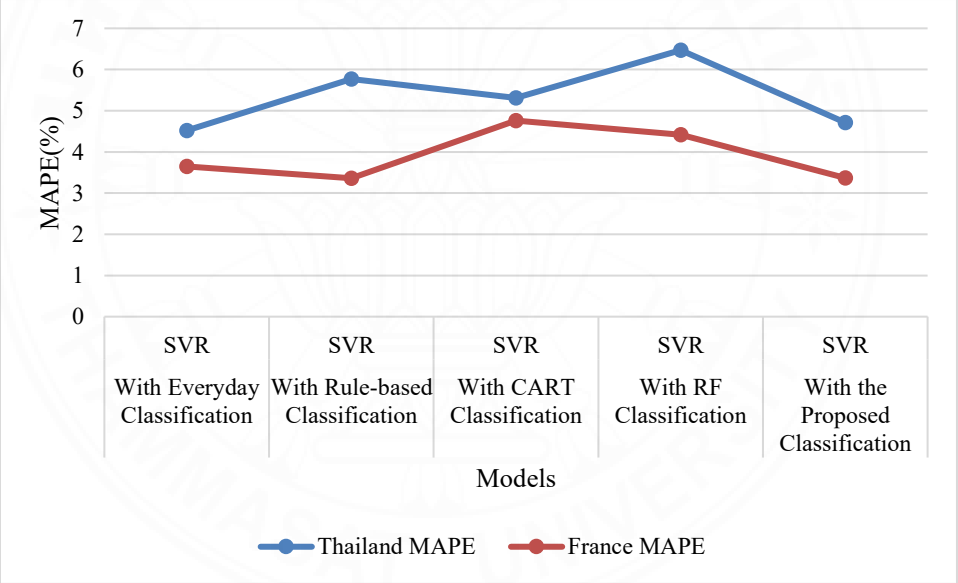

Figure 5.13 Cross-Country MAPE Comparison of SVR Forecasting Models

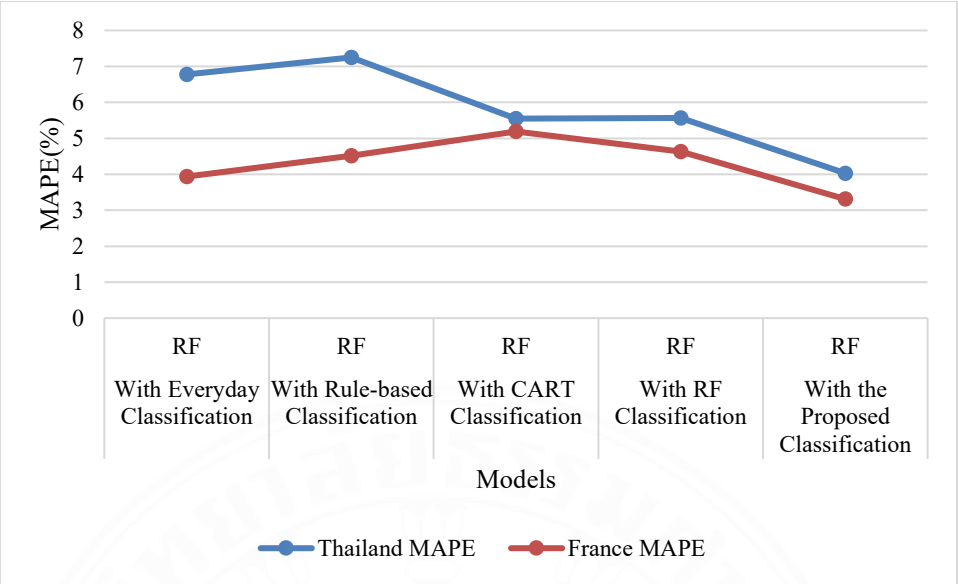

Figure 5.14 Cross-Country MAPE Comparison of RF Forecasting Models

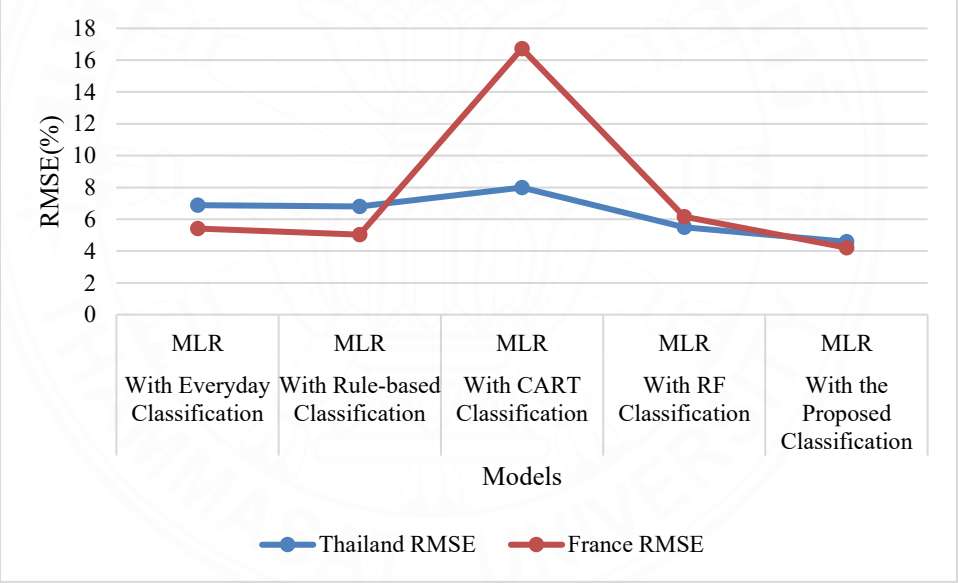

Figure 5.15 Cross-Country RMSE Comparison of MLR Forecasting Models

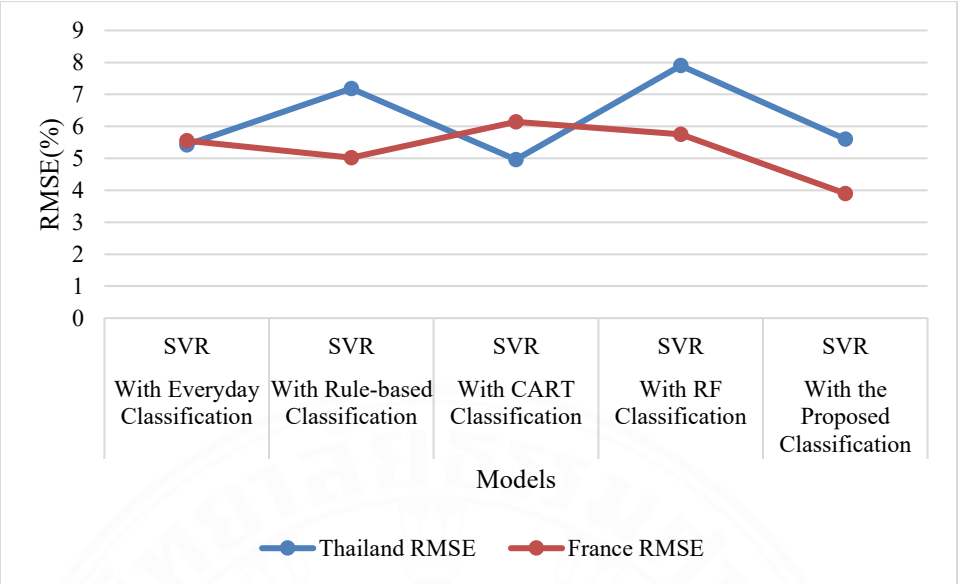

Figure 5.16 Cross-Country RMSE Comparison of SVR Forecasting Models

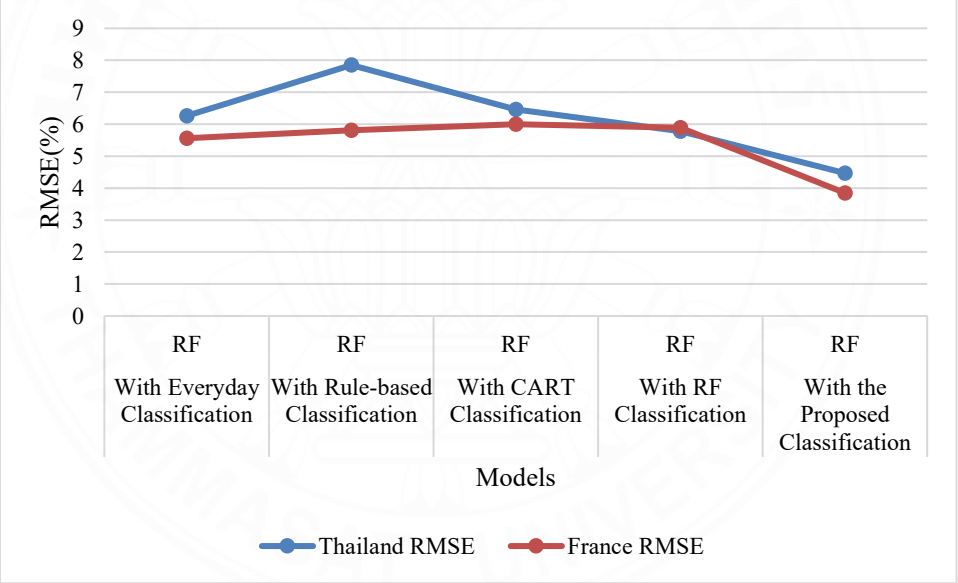

Figure 5.17 Cross-Country RMSE Comparison of RF Forecasting Models

The Average MAPE results reveal that forecasting errors are lowest on weekdays and weekends, and consistently higher on holidays and bridging holidays. This pattern occurs in both Thailand and France, reflecting the inherently irregular load behavior associated with non-working days. The proposed RF-based classification produces the lowest MAPE across all day types, indicating its superior ability to segment training data into behaviorally consistent groups. Traditional schemes such as Everyday and Rule-Based classification perform noticeably worse, as shown by their

higher bars in Figure 5.10 and the cross-country comparisons in Figures 5.12-5.14. For example, MLR and SVR suffer substantial accuracy degradation when paired with these simpler classification methods, particularly for France during the CART and Rule-Based cases, where load volatility differs sharply between seasons. Figure 5.11, which depicts Average RMSE, reinforces the MAPE findings but with an emphasis on the absolute size of prediction errors.

The proposed model again records the smallest RMSE values across all day types, demonstrating that it not only reduces MAPE but also suppresses large deviations between actual and predicted loads. This improvement is noticeable when compared with the RMSE profiles shown in Figures 5.15-5.17. In both Thailand and France, the proposed RF-RF framework achieves the lowest RMSE among all model classification combinations.

Simpler classification strategies, such as Everyday and Rule-Based, exhibit substantially higher RMSE during holidays and bridging holidays, reflecting their limited ability to capture abrupt shifts caused by national events, travel patterns, and seasonal anomalies. CART and RF classification improve stability by incorporating feature-based splits. Still, the RF classification approach consistently outperforms CART because its ensemble structure generalizes across multiple calendar variables more effectively than a single decision tree.

The results collectively show that the proposed RF classification, combined with RF forecasting, consistently provides the most balanced accuracy across all day types, outperforming traditional classification schemes and alternative models. This confirms the importance of calendar-aware segmentation and ensemble learning for robust short-term load forecasting in both countries.

CHAPTER 6
CONCLUSION

This research introduced a unified short-term load forecasting (STLF) framework that integrates calendar-aware classification with machine-learning regression to enhance predictive accuracy under diverse operating conditions. Using two national datasets, Thailand's EGAT half-hourly load profiles and France's ENTSO-E hourly load data. The study evaluated Multiple Linear Regression (MLR), Support Vector Regression (SVR), and Random Forest (RF) under five classification strategies: Everyday, Rule-based, CART, RF, and the proposed hybrid RF-classified RF-forecasting model.

Across both countries, results consistently show that calendar segmentation markedly improves forecasting accuracy compared to approaches that ignore day-type variation. Traditional baselines, particularly Everyday and Rule-based classifications, experience sharp accuracy degradation during holidays and bridging-holidays, reflecting their limited ability to model irregular and event-driven consumption behaviors. France and Thailand both exhibit this challenge, but for different underlying reasons—holiday-related reductions and tourism impacts in Thailand, versus heating-driven fluctuations and working-day variability in France's temperate climate.

The proposed hybrid model demonstrated the most stable and accurate performance across all day types in both countries. RF classification effectively grouped days with similar load signatures, while RF regression captured nonlinear dependencies using lagged load features. The interpolation mechanism for sparse leaf nodes further improved robustness under rare-event conditions, particularly in holiday and bridging-holiday scenarios where training samples are limited. As a result, the hybrid RF-RF framework achieved the lowest average MAPE and RMSE in Thailand. It consistently ranked among the best in France, outperforming MLR and SVR across all classification schemes.

These findings confirm the benefits of integrating ensemble-based segmentation with ensemble regression in a unified forecasting pipeline. Moreover, cross-country results demonstrate the generalizability of the framework: despite

substantial climatic and behavioral differences between Thailand, which is cooling-dominated, tropical, and France, which is heating-dominated, temperate, the proposed method adapts effectively to both systems. This versatility highlights its value for operational forecasting, generation scheduling, demand-response planning, and regional energy management.

In conclusion, the hybrid RF-classification -RF-forecasting model offers a robust, scalable, and interpretable STLF solution capable of handling complex calendar effects and irregular demand patterns across diverse national contexts. It represents a practical advancement for power utilities seeking reliable short-term forecasts under increasingly dynamic electricity consumption conditions.

REFERENCES

Alquthami, T., Zulfiqar, M., Kamran, M., Milyani, A. H., & Rasheed, M. B. (2022). A performance comparison of machine learning algorithms for load forecasting in the smart grid. *IEEE Access, 10*, 48419–48433. https://doi.org/10.1109/ACCESS.2022.3171270

Aprillia, H., Yang, H. T., & Huang, C. M. (2021). Statistical load forecasting using optimal quantile regression, random forest, and risk assessment index. *IEEE Transactions on Smart Grid, 12*(2), 1467–1480. https://doi.org/10.1109/TSG.2020.3034194

Chen, Q., Yang, G., & Geng, L. (2024). Short-term power load combination forecasting method based on feature extraction. *IEEE Access, 12*, 51619–51629. https://doi.org/10.1109/ACCESS.2024.3384246

Cui, J., Wang, J., Chen, H., & Zhang, Y. (2024). Advanced short-term load forecasting with XGBoost-RF feature selection and CNN-GRU. *Processes, 12*(11), 1930. https://doi.org/10.3390/pr12112466

Dudek, G. (2022). A comprehensive study of random forest for short-term load forecasting. *Energies, 15*(20), 7547. https://doi.org/10.3390/en15207547

Fang, Z., Yang, Z., Peng, H., & Chen, G. (2022). Prediction of ultra-short-term power system based on LSTM–random forest combination model. *Journal of Physics: Conference Series, 2387*(1), 012033. https://doi.org/10.1088/1742-6596/2387/1/012033

Fan, G. F., Yu, M., Dong, S. Q., Yeh, Y. H., & Hong, W. C. (2021). Forecasting short-term electricity load using hybrid support vector regression with grey catastrophe and random forest modeling. *Utilities Policy, 73*, 101294. https://doi.org/10.1016/j.jup.2021.101294

Fan, G. F., Zhang, L. Z., Yu, M., Hong, W. C., & Dong, S. Q. (2022). Applications of random forest in a multivariable response surface for short-term load forecasting. *International Journal of Electrical Power & Energy Systems, 139*, 108073. https://doi.org/10.1016/j.ijepes.2022.108073

Gao, J., Wang, K., Kang, X., Li, H., & Chen, S. (2023). Ultra-short-term electricity load forecasting based on an improved random forest algorithm. *AIP Advances,*

13(6), 065112. https://doi.org/10.1063/5.0153550

He, Y., Luo, F., & Ranzi, G. (2022). Transferable model-agnostic meta-learning for short-term household load forecasting with limited training data. *IEEE Transactions on Power Systems, 37*(4), 3177–3180. https://doi.org/10.1109/TPWRS.2022.3169389

Khan, S. A., Rehman, A. U., Arshad, A., Alqahtani, M. H., Mahmoud, K., & Lehtonen, M. (2024). Effective voting-based ensemble learning for segregated load forecasting with low sampling data. *IEEE Access, 12*, 84074–84087. https://doi.org/10.1109/ACCESS.2024.3413679

Lahouar, A., & Ben Hadj Slama, J. (2015). Day-ahead load forecast using random forest and expert input selection. *Energy Conversion and Management, 103*, 1040–1051. https://doi.org/10.1016/j.enconman.2015.07.041

Lee, G. C. (2022). Regression-based methods for daily peak load forecasting in South Korea. *Sustainability (Switzerland), 14*(7), 3984. https://doi.org/10.3390/su14073984

Liu, F., Dong, T., Hou, T., & Liu, Y. (2021). A hybrid short-term load forecasting model based on improved fuzzy C-means clustering, random forest, and deep neural networks. *IEEE Access, 9*, 59754–59765. https://doi.org/10.1109/ACCESS.2021.3063123

Liu, Y., Zheng, R., Liu, M., Zhu, J., Zhao, X., & Zhang, M. (2025). Short-term load forecasting model based on time-series clustering and a transformer in smart grids. *Electronics (Switzerland), 14*(2), 230. https://doi.org/10.3390/electronics14020230

López, M., Sans, C., Valero, S., & Senabre, C. (2019). Classification of special days in short-term load forecasting: The Spanish case study. *Energies, 12*(7), 1253. https://doi.org/10.3390/en12071253

Magalhães, B., Bento, P., Pombo, J., Calado, M. R., & Mariano, S. (2024). Short-term load forecasting based on optimized random forest and optimal feature selection. *Energies, 17*(8), 1926. https://doi.org/10.3390/en17081926

Madhukumar, M., Sebastian, A., Liang, X., Jamil, M., & Shabbir, M. N. S. K. (2022). Regression model-based short-term load forecasting for university campus load. *IEEE Access, 10*, 8891–8905.

https://doi.org/10.1109/ACCESS.2022.3144206

Phyo, P. P., & Jeenanunta, C. (2022). Advanced ML-based ensemble and deep learning models for short-term load forecasting: Comparative analysis using feature engineering. *Applied Sciences, 12*(10), 4882. https://doi.org/10.3390/app12104882

Pinheiro, M. G., Madeira, S. C., & Francisco, A. P. (2023). Short-term electricity load forecasting: A systematic approach from system level to secondary substations. *Applied Energy, 332*, 120493. https://doi.org/10.1016/j.apenergy.2022.120493

Sankalpa, C., Kittipiyakul, S., & Laitrakun, S. (2022). Forecasting short-term electricity load using validated ensemble learning. *Energies, 15*(22), 8567. https://doi.org/10.3390/en15228567

Son, J., Cha, J., Kim, H., & Wi, Y. M. (2022). Day-ahead short-term load forecasting for holidays based on the modification of similar days' load profiles. *IEEE Access, 10*, 17864–17880. https://doi.org/10.1109/ACCESS.2022.3150344

Srivastava, A. K., Pandey, A. S., Houran, M. A., Kumar, V., Kumar, D., Tripathi, S. M., Gangatharan, S., & Elavarasan, R. M. (2023). A day-ahead short-term load forecasting using the M5P machine learning algorithm along with the elitist genetic algorithm and random forest-based hybrid feature selection. *Energies, 16*(2), 867. https://doi.org/10.3390/en16020867

Thu Tun, E. T., Phyo, P. P., & Jeenanunta, C. (2023). Rule-based classification and outlier replacement for daily electricity load forecasting. In *Proceedings of the Asia-Pacific Power and Energy Engineering Conference (APPEEC 2023)* (pp. 1–6). IEEE Computer Society.

Veeramsetty, V., Reddy, K. R., Santhosh, M., Mohnot, A., & Singal, G. (2022). Short-term electric power load forecasting using random forest and gated recurrent unit. *Electrical Engineering, 104*(1), 307–329. https://doi.org/10.1007/s00202-021-01376-5

Wai-Keung Yiu, B., Zhang, T., & Lee, C. W. (2024). Short-term load forecasting using a regularized greedy forest-based ensemble model. *IEEE Access, 12*, 112426–112439. https://doi.org/10.1109/ACCESS.2024.3441642

Yamasaki, M., Freire, R. Z., Seman, L. O., Stefenon, S. F., Mariani, V. C., & Coelho, L. S. (2024). Optimized hybrid ensemble learning approaches applied to very

short-term load forecasting. *International Journal of Electrical Power & Energy Systems, 155*, 109579. https://doi.org/10.1016/j.ijepes.2023.109579

Zhang, Z., Dong, Y., & Hong, W. C. (2025). Long short-term memory-based twin support vector regression for probabilistic load forecasting. *IEEE Transactions on Neural Networks and Learning Systems, 36*(1), 1764–1778. https://doi.org/10.1109/TNNLS.2023.3335355

Zhou, W., Li, Y., Guo, Y., Qiao, X., & Deng, W. (2021). Daily maximum load and its occurrence time forecasting of the distribution network based on the Hausdorff distance and ElasticNet. In *Proceedings of the 3rd Asia Energy and Electrical Engineering Symposium (AEEES 2021)* (pp. 674–678). IEEE. https://doi.org/10.1109/AEEES51875.2021.9403105

APPENDIX

APPENDIX A
PYTHON CODE: RF CLASSIFICATION + LEAF-BASED RF FORECASTING

```
import numpy as np
import pandas as pd
import matplotlib.pyplot as plt

from sklearn.ensemble import RandomForestClassifier, RandomForestRegressor
from sklearn.metrics import mean_absolute_percentage_error, mean_squared_error

# Load dataset
data = pd.read_excel('RF_Data.xlsx')
data['Date'] = pd.to_datetime(data['Date'])
data['Year'] = data['Date'].dt.year
data['Month'] = data['Date'].dt.month

# Train – Test Data
train = data[(data['Year'] == 2019) | (data['Year'] == 2020)]
test  = data[(data['Year'] == 2021)]

# RF Classification (Calendar Inputs)
X_train_cal = train[['MoY','DoW','Hol','BHol']]
y_train_cal = train['Group_true']

X_test_cal  = test[['MoY','DoW','Hol','BHol']]
y_test_cal  = test['Group_true']

clf = RandomForestClassifier(
      n_estimators = 10,
      max_features = 'sqrt',
```

```
        min_samples_leaf = 6,
        bootstrap = False,
        random_state = 42)

clf.fit(X_train_cal, y_train_cal)

# Predicted group
test['Group_pred'] = clf.predict(X_test_cal)

# Convert RF leaf nodes → leaf ID string
def leaf_to_key(arr):
    return "_".join(map(str, arr))

train['Leaf_ID'] = np.apply_along_axis(leaf_to_key, 1, clf.apply(X_train_cal))
test['Leaf_ID']  = np.apply_along_axis(leaf_to_key, 1, clf.apply(X_test_cal))

# Train RF Forecasting Models Per Leaf
feature_cols = ['X1','X2','X3','X4','X5']
leaf_models = {}

for leaf_id, group in train.groupby('Leaf_ID'):
    if len(group) < 6:      # skip small leaves
        continue
    Xg = group[feature_cols]
    yg = group['Y']

    reg = RandomForestRegressor(
            n_estimators = 10,
            max_features = 'sqrt',
            min_samples_leaf = 6,
            bootstrap = False,
            random_state = 42)
```

```
    reg.fit(Xg, yg)
    leaf_models[leaf_id] = reg

# Global model for fallback
global_reg = RandomForestRegressor(
        n_estimators = 10,
        max_features = 'sqrt',
        min_samples_leaf = 6,
        bootstrap = False,
        random_state = 42)

global_reg.fit(train[feature_cols], train['Y'])

# Forecast for each test day
pred_list = []
true_list = []
month_list = []
group_true_list = []

for i, row in test.iterrows():
    leaf = row['Leaf_ID']
    x = row[feature_cols].values.reshape(1,-1)

    if leaf in leaf_models:
        y_hat = leaf_models[leaf].predict(x)[0]
    else:
        y_hat = global_reg.predict(x)[0]

    pred_list.append(y_hat)
    true_list.append(row['Y'])
    month_list.append(row['Month'])
```

```
    group_true_list.append(row['Group_true'])
# Evaluation Metrics
overall_mape = mean_absolute_percentage_error(true_list, pred_list)*100
overall_rmse = np.sqrt(mean_squared_error(true_list, pred_list))

print("MAPE:", overall_mape)
print("RMSE:", overall_rmse)

# Monthly accuracy
res = pd.DataFrame({
    'Month': month_list,
    'Y_true': true_list,
    'Y_pred': pred_list,
    'Group_true': group_true_list
})

monthly = res.groupby('Month').apply(
    lambda g: mean_absolute_percentage_error(g['Y_true'], g['Y_pred'])*100
)

group_acc = res.groupby('Group_true').apply(
    lambda g: mean_absolute_percentage_error(g['Y_true'], g['Y_pred'])*100
)
# Plot Monthly MAPE
plt.figure(figsize=(8,4))
plt.plot(monthly.index, monthly.values, marker='o')
plt.title("Monthly MAPE (2021)")
plt.xlabel("Month")
plt.ylabel("MAPE (%)")
plt.grid(True)
plt.show()
```

```
# Plot Load-Group MAPE
plt.figure(figsize=(7,4))
plt.bar(group_acc.index, group_acc.values)
plt.title("Load Group MAPE (2021)")
plt.ylabel("MAPE (%)")
plt.grid(axis='y')
plt.show()
```

BIOGRAPHY

Name	May Thazin Phuu Wai
Education	2021: Bachelor of Engineering (Electrical Power Engineering) Thanlyin Technological University

Publications

Phuu Wai, M. T., Dumrongsiri, A., Jeenanunta, C., Thu Tun, E. T., Shwe, M. N., & Dhippayom, T. (2024). Short-term Electricity load forecasting using rule-based load classification and random forest load classification: A focus on calendar event. Proceedings of *9th International Conference on Sustainable Energy and Environment (SEE 2024): Securing a Sustainable Net-Zero Future Now*.

Chhom, P., Thu Tun, E. T., Chanyachatchawan, S., Phuu Wai, M. T., Islam, A. K. M. M., Patchotchai, N., & Jeenanunta, C. (2025). *Interpretable day-ahead forecasting with calendar-based classification and group-based regression across climatic zones*. Proceedings of *the 20th International Joint Symposium on Artificial Intelligence and Natural Language Processing (iSAI-NLP 2025).*